EXPERIMENTAL STUDY OF AN AXISYMMETRIC TURBULENT BUOYANT PLUME.

PART I: NEUTRAL ENVIRONMENT

Aamir Shabbir and William K. George

Department of Mecahnical and Aerospace Engineering
University of Buffalo,SUNY
Buffalo, NY 14260

ABSTRACT

Velocity and temperature fields were measured in an axisymmetric turbulent buoyant plume using two wire and three wire probes. The ambient was monitored using thermocouples placed at different heights to make sure that the facility was not stratified. The axisymmetry of the flow was checked using a planer array of sixteen thermocouples. The measurements satisfy both the integral and differential forms of the mean momentum and energy equations within experimental error. The rates of thermal and mechanical energy dissipation were obtained as the closing terms in balances of the turbulence kinetic energy and temperature variance equations.

1. INTRODUCTION

1.1 Historical Review

Due to the complex nature of turbulence, the correct experimental approach is to think of model experiments which isolate a particular physical aspect of the phenomenon. Besides lending insight into the physics, such experiments also augument the theoretical development of the subject by verifying various theories and mathematicl models. The laboratory plume is one such flow which allows us to study the effect of buoyancy on turbulence.

Buoyancy plays an important role in a number of fluid flows of environmental and technological importance. Some of examples are: vertical motion of air in the atmosphere, spreading of the smoke and other pollutants in the atmosphere, dispersal of volcano exhaust and water outfalls. The buoyancy force in such flows can either be caused by a heat source, as in a smoke stack, or it can be caused by introduction of lighter (or heaviour) fluid into another fluid, as in a water outfall. Once the fluid is set into motion , the velocity field affects the thermal field, and vice-versa. The initial state of laminar motion very quickly changes into turbulence and the flow starts to spread radially by entraining ambient fluid into the main flow. As long as the density differences between the flow and the ambient are small, as compared to some reference density in the flow, it has been believed that all plumes can be shown to be dynamically similar, regardless of the kind of the source. (Note that this has recently been disputed by George 1986 who presents arguments to show that the flow never becomes independent of its initial conditions.)

In the analysis of such flows the ambient is assumed to be at rest. If it's temperature does not change with height the environment is termed as

neutral. If the temperature increases with the height the environment is called unstable and provides an additional source of buoyancy force. In the stable environment the temperature decreases with height and the growth of the plume is suppressed.

The plume has been the subject of study since the similarity analysis of Zel'dovich (1937). Schmidt (1941) used mixing length type hypotheses to obtain expressions for the velocity and temperature profiles for both plane and axisymmetric plumes and compared the results with his own measurements.

Batchelor (1954) proposed similarity solutions for turbulent plumes for both the plane and the axisymmetric geometries in neutral and stratified environments. For an axisymmetric plume in a neutral environment, the mean vertical velocity and buoyancy field was shown to be given by

$$f(\eta) = F^{-1/3}\, z^{1/3}\, f_1(r/z) \qquad (1.1)$$

$$t(\eta) = F^{-2/3}\, z^{5/3} g\beta\Delta T\, t_1^*(r/z) \qquad (1.2)$$

where F is the rate at which buoyancy is added at the source, z is the height, and where the functions f_1 and t_1 are to be determined from experiments. Batchelor discarded the solution for stably stratified environments, arguing that these were physically unrealistic. His conclusions were disputed by George and Beuther (1982) on physical grounds and they showed measurements of plumes in stably stratified environments which collapsed in similarity variables to substantiate their claim.

Morton, Taylor and Turner (1956) extended the analysis to non-similar situations by assuming that the entrainment rate was proportional to some local characteristic velocity and obtained numerical solutions. They obtained the entrainment constant from the experiments and made predictions of the

height to which plumes can rise under the different ambient conditions. Morton (1959) also using an entrainment hypotheses analysed plumes arising from sources of buoyancy, momentum and mass and showed that these are equivalent to point sources of buoyancy only, a fact now disputed by George 1986. List and Imberger (1973) and Baker (1980) argued that the entrained coefficient could not be constant for the buoyant jet, and called Morton's results into question.

Rouse, Yih and Humpherys (1952) also obtained the similarity relation for the two dimensional and axisymmetric plumes and experimentaly verified their fuctional forms. They generated plumes by using gas burners arranged in the appropriate formation, and then used thermocouples and wind-vane anemometers to measure the mean buoyancy and vertical velocity . Their results for the axisymmetric case are given by

$$f(\eta) = 4.7/[1+55\eta^2]^2 \qquad (1.3)$$

$$t(\eta) = 11.0/[1+30\eta^2]^2 \qquad (1.4)$$

More recently Rao and Brzustowski (1969) generated a plume by a burning wick heat source, and measured the velcity field by using a hot wire an quasi-linearization.

The first attempt to measure the mean and turbulence quantities using hot-wire anemometry with modern digital techniques was by George, Alpert and Tamanini (1977). A two wire probe was used to measure the temperature and velocities, and the corresponding similarity profiles were given by

$$f(\eta) = 3.4 \exp(-55\, r^2/z^2) \qquad (1.5)$$

$$t(\eta) = 9.1 \exp(-65\, r^2/z^2) \qquad (1.6)$$

These are substantially different from those measured by Rouse et al. (1952). The rms values of temperature and velocities were found to be 40% and 28% respectively. The correlation coefficient between the temperature and vertical velocity was found to be 0.6 - 0.7, a result believed to be reasonable in plumes where the velocity and temperature field strongly influence each other. It was also found that about 15% of the total vertical heat transport was contributed by the fluctuations. Nakagone and Hirata (1975) also made similar measurements in an independent effort, but obtained lower values of the rms values of temperature and velocity (33% and 26% respectively) and also obtained a lower value for the vertical velocity temperature correlation coefficient of 0.45.

Beuther (1980) used a cross-wire to measure up to fourth moments for an axisymmetric plume. His measurements were taken in a stably stratified environment in which temperature increased with height and , therefore can not e compared with those cited above. For the sake of completeness his results are summarized below.

$$f(\eta^2) = 3.8/[1+46\eta^2]^2 \qquad (1.7)$$

$$t(\eta^2) = 10.4/[1+31\eta^2]^2 \qquad (1.8)$$

The temperature and velocity intensities were 38% and 28% at the centerline. The various balances were also computed to establish the accuracy of the experiment.

Although the similarity has been well established in all experiments, there is still some disagreement about the centerline values of the mean profiles and the spreading rates. Chen and Rodi (1980) reviewed the existing

experimental data on plumes and recommended profiles which were very close to those of George et al. (1977).

List (1982) in his review suggests that all the measurements in the axisymmetric geometry have not been taken in the fully developed region. He also points out that none of these studies equated the integrated buoyancy flux with the source buoyancy flux. The buoyancy flux F, which directly appears in the similarity relations, was obtained in these studies by integrating the measured temperature and velocty profiles. This could be in error since the probes used, hot wires, do not have the ability to resolve flow reversals believed to be present at the outer edges of the flow. This in turn will give erroneous similarity profiles of both buoyancy and velocity.

In parallel to these experimental investigations there have also been various theoretical efforts to model and close the equations of motion for flows dominated by buoyancy. The appropriate equations of motion for these are the Navier Stokes and the energy equation, but it is still beyond the power of computers to solve them. The altenative approach is to solve the time averaged equations in which the extra unknowns introduced by averaging are modeled. The evalution of the constants and the models has to be done against experiments. This modelling can be carried out at various levels. The most popular of these are the eddy viscosity and the k-e models. Reynolds stress models in which the transport equations for the Reynolds stress are solved are still in the development stage. For buoyancy dominated flows, the k-e models are discussed and reviewed by Launder (1970) and Hossian and Rodi (1985). The second order models have been proposed and discussed by Lumley and Zeman (1974), Lumley, Zeman and Siess (1977), and Launder (1975).

1.2 Objectives of the Present Work

From the above survey it is clear that there is no comprehensive set of data on neutral environment round plumes which can resolve the various differences in the various experiments and also provide a means for verifying various turbulence models.

The first objective of this study was to resolve whether, in fact, an axisymmetric plume experiment could be carried out which conserves buoyancy by carrying out the measurements while source conditions were being monitored. Since for an ideal gas in a neutral environment the conservation of energy also implies the conservation of buoyancy (see Chen and Rodi 1980) the best way of calculating F is at the source. In the present experiment source conditions were carefully monitored to calculate the buoyancy parameter F_0. (All the profiles presented in this study are normalized by this F_0).

The second objective of this work is to measure the various moments up to fourth order so that the turbulence kinetic energy and temperature variance balances can be carried out. The mechanical and thermal dissipations are obtained as the closing entries in these balances. These balances show how the energy is budgeted and which terms or physical phenomena dominate the different regions of the flow. They also provide a data base for evaluating various turbulence models and closure assumptions. Obviously various hot wire errors will affect the measurements of the moments, but it is believed that in the central core of the flow where the turbulence intensities are small, these errors will be small.

2. THE BASIC EQUATIONS AND CONSTRAINTS

2.1 Mean Momentum and Energy Equations

For an incompressible fluid flow the governing equations, after invoking the thin shear layer assumptions and neglecting the viscous diffusion terms, are given as

$$\frac{\partial U}{\partial r} + \frac{1}{r}\frac{\partial (rV)}{\partial r} = 0 \qquad (2.1)$$

$$U\frac{\partial U}{\partial z} + V\frac{\partial U}{\partial r} = -\frac{1}{r}\frac{\partial}{\partial r} r\overline{uv} - g\frac{\Delta\rho}{\rho} \qquad (2.2)$$

$$U\frac{\partial T}{\partial z} + V\frac{\partial T}{\partial r} = -\frac{1}{r}\frac{\partial}{\partial r} r(\overline{vt}) - \frac{\partial}{\partial z}\overline{ut} \qquad (2.3)$$

Density has been treated as a constant except where it appears in the body force (the Boussinesq approximation). For small density differences, $(\rho_\infty - \rho)$ can be expanded in power series of $(T - T_\infty)$ and $(p - p_\infty)$ as

$$\rho \simeq \rho + \left.\frac{\partial \rho}{\partial T}\right|_{p} (T - T_\infty) + \left.\frac{\partial \rho}{\partial p}\right|_{T} (p - p_\infty) \qquad (2.4)$$

The second term is negligible for gravitational motion. Using

$$\beta = \frac{1}{\rho}\left.\frac{\partial \rho}{\partial T}\right|_{p} \qquad (2.5)$$

equation (2.4) reduces to

$$\frac{\rho - \rho_\infty}{\rho} = -\beta\Delta T \qquad (2.6)$$

for small differences in temperature (compared to the absolute temperature).

For ideal gases

$$\beta = \frac{1}{\rho}\left.\frac{\partial \rho}{\partial T}\right|_{p} = \frac{1}{T} \qquad (2.7)$$

If the ambient temperature T_∞ is assumed constant, the advection terms in the energy equation (2.3) can be written in terms of buoyancy $g\beta\Delta T = T-T_\infty$ rather than T. With all these assumptions the energy and momentum equations can be re-written as

$$U\frac{\partial U}{\partial z} + V\frac{\partial U}{\partial r} = -\frac{1}{r}\frac{\partial}{\partial r}(r\overline{uv}) + g\beta(T-T\infty) \qquad (2.8)$$

$$U\frac{\partial}{\partial z} g\beta(T-T_\infty) + V\frac{\partial}{\partial r} g\beta(T-T_\infty) = -\frac{1}{r}\frac{\partial}{\partial r} r(g\beta\overline{vt}) - \frac{\partial}{\partial z}\overline{ut} \qquad (2.9)$$

The similarity relations for the mean buoyancy and velocity were given by Batchelor (1954). For the axisymmetric geometry the terms in equations (2.8) and (2.9) can be shown to be given in similarity form by

$$\eta = r/l(z) \qquad g\beta(T-T_\infty) = T_s t(\eta)$$
$$U = U_s f(\eta) \qquad g\beta ut = U_s T_s h_1(\eta) \qquad (2.10)$$
$$g\beta\overline{vt} = U_s T_s\, h_2(\eta) \qquad \overline{uv} = U_s^2 r_1(\eta)$$

When these are substituted in the original equations of motion the results are

$$-\frac{1}{3} f^2 - \frac{5}{3}\frac{f}{\eta}\int_0^\eta f\eta\, d\eta = -\frac{1}{\eta}\frac{\partial}{\partial\eta}(\eta\Sigma) + t \qquad (2.11)$$

$$-\frac{5}{3} ft - \frac{5}{3}\frac{t}{\eta}\int_0^\eta f\eta\, d\eta = -\frac{1}{\eta}\frac{\partial}{\partial\eta}(\eta h_2) - (2h_1 + \eta h_1) \qquad (2.12)$$

2.2 Integral Constraint.

If the energy equation (2.3) or (2.9) is integrated across the flow one obtains

$$F = 2\pi\int g\beta[U_s(T-T\alpha) + ut]rdr \quad = \text{constant} = F_o \qquad (2.13)$$

where F_0 is the rate at which buoyancy is added at the source. This reduces in similarity variables to

$$F = 2\pi\int[ft + h_1]\eta d\eta \qquad (2.14)$$

This integral constraint implies that for an ideal gas plume in a neutral environment both the energy (enthalpy) and the buoyancy is conserved. This integral constraint must be satisfied by any experiment to within the experimental error. It will be shown in Chapter 4 that the present experiment satisfies this constraint within 5-10% .

2.3 Stratification of the Ambient

If the ambient temperature T_∞ changes with height (i.e. $T_\infty = T_\infty(z)$), then the equation (2.3), when written in terms of $\Delta T = T - T_\infty$ becomes

$$U\frac{\partial}{\partial z}g\beta(T-T_\infty) + V\frac{\partial}{\partial r}g\beta(T-T_\infty) = -\frac{1}{r}\frac{\partial}{\partial r}r(g\beta\overline{vt}) - \frac{\partial}{\partial z}g\beta\overline{ut} - U\frac{d}{dz}g\beta T_\infty \qquad (2.15)$$

The extra term $U\, dT_\infty/dz$ is due to the ambient stratification .

Integrating the above relation gives the following integral constraint

$$\frac{d}{dz}\int_0^\infty(g\beta\Delta T + \overline{ut}) = -g\beta\frac{dT_\infty}{dz}2\int_0^\infty Urdr \qquad (2.16)$$

We immediately see that for the neutral environment the right hand side is zero and the above relation reduces to equation (2.13)

In laboratory simulations of plumes some degree of stratification is

always present. This is because of the finite size of the facilities and the fact that experiments typically have to be carried over a number of hours to achieve statistical convergence of the data because of the slow time scales of these flows. As a consequence, an inversion layer builds near the ceiling and may or may not reach an equilibrium height above the zone of measurement.

Equation (2.16) provides us with a criteriaon to determine if a particular ambient can be regarded as stratified or not. Multiplying equation (2.18) by z/F to make it dimensionless we have

$$\frac{z}{F_0}\frac{dF}{dz} = -\frac{z}{F_0} g\beta\frac{dT}{dz}\int_0^{\infty} 2\,U\,r\,dr \qquad (2.17)$$

For a neutral environment $(z/F_0)\,dF/dz = 0$. For a laboratory simulation of a neutral environment we must have $(z/F_0)\,dF/dz \ll 1$ to insure that buoyancy integral is nearly independent of height as required for the neutral case. In section 4 it will be shown that the above criteriaon is satisfied for the present experiment.

2.5 Temperature Variance and Turbulence Kinetic Energy Equations

The equation for temperature fluctuation $\overline{t^2}$ can be obtained by writing the equation for instantaneous temperature, then subtracting the equation for mean temperature, multiplying the resulting equation by t, and then averaging. The final result is

$$U\frac{\partial}{\partial z}(\overline{t^2}/2) + V\frac{\partial}{\partial r}(\overline{t^2}/2) = -(\overline{ut}\frac{\partial}{\partial z}T - \overline{vt}\frac{\partial}{\partial r}T)$$

Advection Production

$$-\frac{1}{2}\left[\frac{\partial}{\partial z}\overline{ut^2} + \frac{1}{r}\frac{\partial}{\partial r}(\overline{rvt^2})\right] - \epsilon_t \qquad (2.18)$$

Diffusion — Dissipation

The turbulence kinetic energy can be obtained by contracting the Reynolds stress ($\overline{u_i u_j}$) equation (Tennekes and Lumley 1972) with the result is

$$U\frac{\partial\overline{q^2}}{\partial z} + V\frac{\partial\overline{q^2}}{\partial r} = -\frac{\partial}{\partial z}(\overline{up/\rho} + \overline{q^2 u}) - \frac{1}{r}\frac{\partial}{\partial r}[r(\overline{up/\rho} + \overline{q^2 v})]$$

.1h 8

Advection — Axial Transport — Radial Transport

$$-\overline{u^2}\frac{\partial U}{\partial z} - \overline{uv}\frac{\partial U}{\partial r} - \overline{uv}\frac{\partial V}{\partial z} - \overline{v^2}\frac{\partial V}{\partial r} + g\beta\overline{ut} - \epsilon \qquad (2.19)$$

Production — Dissipation

The mechanical and thermal dissipation rates will be obtained by balancing these equations against experimental data.

3. DESCRIPTION OF THE EXPERIMENT AND EXPERIMENTAL TECHNIQUE

3.1 The Plume Generator

The plume generator is the same as that used by George et al (1977) and by Beuther and George (1982) (see also Beuther 1980). The heat source consisted of sintered bronze discs which were heated with eight electric heaters 1500 watt Watlow fire cartridges). Air, from a compressed air line, was passed through these heated discs, and then passed through a set of screens, and finally exited through a 12:1 contraction nozzle. The screens and contraction resulted in an exit profile which was uniform outside the wall boundry layer to within 2 % . The turblence intensity at the exit was typically 0.5 %. The space between the outer casing and the nozzle assembly was filled with silica gel for insulation

purposes. The outer shell was made of sheet metal.

A feedback thermocouple, placed at the exit, was connected to the Electromax temperature controller. Under typical operating conditions, about two hours were required for the generator to reach thermal equlibrium. However, data collection was not started until after the plume has beeen running for about four hours. The variation in the exit temperature was ± 1 ^{o}C over this period compared to a nominal operating value of 300 ^{o}C above ambient.

The plume generator was covered with a wooden sheet (2m X 2m) so that the facility corresponded to air ejecting out of a hole in a floor. A square screen enclosure was placed around the plume, 2m X 2 m in cross section and 5 meter in height. This was far enough from the plume itself to prevent of any hinderence to the flow by the criterion established in Chapter 2.

The dimensions of the room housing the facility were 6 X 6 X 10 meters and the room was completely shut off for the duration of the experiment. This was done to prevent the flow being disturbed from cross drafts which might arise from the HVAC system. A flow visulization study was also carried out to confirm that there has no plume drift or anomalous behavior.

3.2 Instrumentation

Two kinds of hot wire probes were used to measure the velocity and temperature fields. The first was a two wire parallel probe (DISA 55P76) and is shown in figure 2 (a). The leading wire was used as a resistance probe to measure the temperature. This had a diameter of 1 micron and a sensitive wire length of 1.2 mm. It was operated in the constant current mode with a heating current of 0.3 milliamperes to ensure that its velocity response was

negligible. The bottom wire was used with a constant temperature anemometer DISA 55M10 to measure velocity. The sensor had an overall length of 3 mm. It was etched at the center to give an effective length of 1.25 mm and a diameter of 5 ;m. In order to get an optimum respose to both the velocity and the temperature from this wire, an overheat ratio of 0.4 was used.

The second probe used was a combination of a cross-wire and a temperature wire as shown in figure 2 (b). The temperature wire was again 1 micron in diameter and was heated with a current of 0.15 milliamperes. The x-wires were made of 5 micron gold-plated wire and had an l/d of 125. All the velocity sensors were operated in the constant temperature mode using DISA 55M anemometer systems. For the temperature wire the 55M20 bridge was used with the 55M01 system.

To check the axisymmetry of the flow and to find the center of the plume, an array of sixteen thermocouples was used which were arranged in the 4 X 4 grid. The thermocouple scanner used for acquiring data from these thermocouples was made using four millivolt conditioners manufactured by Analog Devices (Model 2B54A). These conditioners were specially designed for thermocouple applications. A gain of 1000 was employed so that the millivolt signal from the thermocouples was converted into volts. The scanner was driven by TTL logic and was interfaced with a PDP 11/34. The output from the scanner was sampled and digitized using a 16 bit A/D converter. The scanner permitted taking as many as 400 samples per second, however, the fastest rate used in the experiments was 32 samples per second. All the thermocouples used in the experiment were Copper-Constantan and were ice referenced.

The outputs from all the anemometers and signal conditioners were digitized by an 16 bit A/D converter interfaced with the PDP 11/34. The

voltages were recorded on a magnetic disk for later data conversion.

3.3 Calibration Schemes

The constant current wire gave a linear response to temperature change. Since for the velocity wire the output voltage is a funcion bo velocity and temperature it was handled by expressing the wire Nusselt number as a function of the Reynolds number. In particular

$$Re = \sum_{n=0}^{4} A_n \, Nu^{n\ 2} \qquad (3.1)$$

The temperature coefficients A_n are temperature independent, teh temperature dependence entering through the Nusselt number. For angle response of the x-wire a Champagne-type relation was used which incorporated a velocity-dependent k-factor i.e.

$$Ueff/U_0 = [\cos^2\phi + k^2(U_0) \sin^2\phi]^{1\ 2} \qquad (3.2)$$

Note that k was found to be dependent o the velocity vector U_0 at the flow velocities encountered in this experiment. For details of these calibrations see George et. al (1987), Beuther et. al.(1987).

The calibration of the hot wires was carried out at the exit of the plume generator where it was possible to get the desired velocities and temperatures. It was found to be more efficient to first heat the plume generator to a particular temperature, and then vary the velocities starting from a smaller velocity and going up to higher. Whenever the velocity and temperature were changed, sufficient time was provided for the plume generator to reach thermal equilibrium. The reference temperature was obtained with a Copper Constantan thermocouple at the source and the reference velocity was obtained by doing the mass balance on a rotometer in the inlet line which in

turn was calibrated using the wet-meters and LDA.

Calibration of the wires was done both before and after the experiment. Normally the velocity calibrations were found to be very stable. However the temperature wire was sometimes found to drift appreciably, presumably related to the stability of the DISA 55M20 bridge. All such data was discarded.

3.4 Errors in the Measurements

There are three primary sources of error in a x-wire signal at low velocities; rectification, cross-flow and lack of directional sensitivity at higher inclinations. The problem of rectification is obvious for a single wire in which the flow must reverse its direction for rectification to occur. Tutu and Chevray (1975) have pointed out that rectification errors are more subtle and serious for x-wires than for single wires. They also show that the combined effects of rectification and cross-flow lead to the under-estimation of the second and higher moments.

An additional manifestation of the rectification phenomenaon is the occurrence of voltage pairs which could not be resolved into velocity pairs from the angle calibration. In other words, the instantaneous voltage pairs obtained do not lie in the calibrated region and can not be inverted by equation (3.2). For such data, the word ''dropout'' is probably a more accurate description than ''rectification''. Dropout is usually caused by a high intensity in the u or v component and is especially troublesome when the mean velocity is low. As noted by Beuther (1980) ''This is because wires are fairly insensitive to direction at low velocities and any small measurement error (electronic noise, prong support interference, velocity component perpendicular to the x-wire plane, wake of one wire or, another, or a velocity

or temperature gradient between the wires) can create a large error in the output''. The dropout is small at the center of flows such as plumes but has been observed to be as big as 40% at the outer edges.

Since the dropped data points are associated with the low velocities, its net effect would bias the velocities toward the higher end. Whether this results in the overestimation of higher moments or not is a difficult question to answer. It should also be noted that the like dropout, the flow reversals on the wire are also associated with low mean velocities and by dropping such data points one might be reducing the rectification errors.

From the above discussion it is clear that it is very difficult to quantify the various hot wires errors. As a word of caution it is recommended that all the higher moments must be interpreted carefully beyond $\eta = 0.1$ where turbulence intensities begin to increase significantly.

4. RESULTS

4.1 Source Conditions

Figure (3) shows the hot air exiting from a nozzle of diameter 6.35 cm in a Scheiron photograph of the flow at the source. The dark area at the bottom is the exit of the nozzle. It is clear that the flow is not laminar after about one diameter. Source conditions for the single wire and x-wires are given in Table I. The two experiments these differ by a small amount (10%). Since both the momentum and buoyancy are added at the source, the flow near the source is more like a buoyant jet and not a plume. However as the air moves up vertically and the flow develops, the buoyancy overwhelms the momentum added at the source. After a certain distance from the source the

flow is governed by the buoyancy alone. How far away this happens is determined by the source conditions.

Kotsovinos(1977) and Baker (1980) have defined a buoyancy length scale L based on the source buoyancy and momentum to characterize this distance

$$L = M^{3/4}/F_0^{1/2} \qquad (4.1)$$

Fig (4) taken from Baker (1980) shows that the buoyant jet has reached an asymptotic plume like condition for $\xi > 5$ where $\xi = z/L$. For the source conditions of this study, this criteria is met as shown by the points plotted on the same figure.

An accurate knowledge of the source conditions is also essential to check whether or not the experiment conserves buoyancy. Also this rate at which buoyancy is added at the source appears in all the similarity relations for velocity. In view of the fact that plumes in stratified environments also satisfy similarity relationships using the local buoyancy integral, it is more accurate to use the source buoyancy which must be conserved for the neutral environment than one obtained by integrating the hot wire measured velocity and temperature profiles.

4.2 Ambient Conditions

Beuther and George (1982) and Beuther (1980) have shown that a small stratification of the ambient can cause a significant loss or gain of buoyancy. This can appreciably change the shape of profiles. In the experiment of Beuther (1980) the ambient was stably stratified and the data collapsed in the similarity variables when the local value of the buoyancy

flux was used.

Almost none of the studies reported in the literature have monitored or documented changes in the ambient temperature. In the present experiment the ambient was continuously monitored using seven copper-constantan thermocouples placed at different heights. Figure (5) shows the change in ambient temperature both as a function of height and time. It is seen that for the first two hours of operation a significant change in the temperature results. However, after this it changes very little, especially over the heights where the measurements were taken.

According to the criteria established in section 2.3 to avoid stratification effects,

$$2\frac{z}{F_0}\ g\beta\ \frac{dT}{dz}\int_0^{\varphi} U\ r dr \ll 1 \qquad (4.2)$$

For this experiment the value of the above relation is .003 which is very small as compared to 1. For the experiment of Beuther (1980) the value of above relation is 0.36. Based on these we can confidently say that the measurements reported herein are taken in the neutral environment.

4.4 Single Wire Measurements

The mean buoyancy profile is shown in figure (5). The Gaussian shown is the one suggested by George et al. (1977) from their measurements who used the same instrumentation but calculated the buoyancy parameter by integrating the measured velocity and temperature profiles. The centerline value is 9.4 which slightly higher than the 9.1 recommended by George et. al. If like them our buoyancy profile is normalized by the local buoyancy its centerline value will

be 9.0 . The mean vertical velocity has a value of 3.2 at the centerline as compared to 3.4 measured by George et. al. Half widths of both the velocity and temperature is about η = 0.1.

The centerline turbulent intensities of temperature and velocity are 40% and 32% respectively. The latter is higher than what most of the workers measured and remains alomost constant up to η = 0.07. These are plotted in the similarity variables in figures 8 and 9. These are close to the value of 38% and 28% measured by George et al. whose lower values may be attributed to the fact that their measurements were somewhat closer to the source and may not have been quite fully developed. The cross-correlation coefficient between the temperature and the vertical velocity is around 0.68 showing a strong influence of temperature and velocity fields on each other. It confirms the value of 0.67 measured by George et al. and indicates that the value of 0.46 measured by Nakagone and Hirata (1977) is probably low as suggested by Beuther (1970). When plotted in the similarity variables ut peaks at about η = 0.04 which was not clear in George et al. because of the scatter and the manner in which the data were plotted, but was observed by Beuther (1980).

The local values of buoyancy at different heights were obtained by carrying out the following integration

$$F\ (\text{local}) = 2\pi \int_0^\infty g\beta(U\Delta T + \overline{ut})rdr \qquad (4.3)$$

For a neutral environment plume of an ideal gas this should remain constant with height. Figure (11) shows the ratio of this local buoyancy to the source buoyancy at various heights. It is clear that the buoyancy is conserved within 5% which is within the experimental errors. This is the first time that such a

check has been carried for an axisymmetric plume and gives more confidence to the measurements and completes the first objective of the study.

Based on the mean profile measurements we recommend the following buoyancy and velocity profiles for an axisymmetric turbulent buoyant plume in a neutral environment.

$$t = 9.4/[1+28\eta^2]^2 \qquad 9.4 \exp(-69\eta^2) \qquad (4.4)$$

$$f = 3.2/[1+28\eta^2]^2 \qquad 3.2 \exp(-57\eta^2) \qquad (4.5)$$

These are about the same as recommended by George et al. (1977) and by Baker et al. (1980), Baker (1980) and George (1980). This completes the first objective of the study.

4.5 X-Wire Measurements

The use of x-wires allows the measurement of two velocity components, and hence various cross correlations between them and temperature can be calculated. These are very important in balancing the transport equtions of various quantities.

The mean buoyancy profile is the same as measured with a two wire parallel probe with a centerline value of 9.4. Again the Gaussian curve shown is not the fit to the present data but is the one suggested by George et. al. (1977) and is reproduced here for comparison. The data collapse is very reasonable, and gives confidence that the plume is fully developed at the locations where the measurements are taken.

The mean velocity profile shown in figure (13) is again about the same as measured with a single wire except at outer edges where it is somewhat

higher. The differences are due to the poor directional response of x-wires at the lower velocities, the differing cross-flow and rectification errors between single and x-wire probes. This point will be further discussed in Chapter 4.8.

The measured radial component of the velocity profile, also plotted in figure (13) is very small. This can also be obtained from the continuity equation by integrating the measured vertical velocity i.e.

$$V = -\frac{1}{r}\int_0^r \frac{\partial U}{\partial z}\, r dr \qquad (4.6)$$

U is fitted with a polynomial or Gaussian expression as in equation (4.4) and (4.5) of the preceeding section, , the above relation in the similarity variables reduces to

$$k = (1/6)\eta - (5/6)A\eta^3 \qquad (4.7)$$

The resulting profile shows that it becomes negative (directed radially inwards) after $\eta = 0.1$ where as the measured one does not. The difference can be attributed to the small values of V (which is of order δ/L) and the relatively large hot wire cross-flow errors which are of the same order.

The various second moments are shown in figures (14) through (19). The mean square values of temperature are about the same as measured with a single wire. The profile of $\overline{u^2}$ is about the same as measured with a single wire except at around η =0.2 where the x-wire measurement is slightly higher, and the reason probably being the poor directional response of the x-wire at low velocities and the dropout phenonmena to be discussed latter in this chapter. The centerline value of the $\overline{v^2}$ is about 70% of the u. The curves shown are the best fits to the data, the equations for which are tabulated in Table I along with those for the higher moments.

The centerline value of the ut correlation is 1.85, and is slightly lower than the one obtained from a single wire. The correlation does show an off axis peak as observed in the single wire measurements. The radial heat flux vt , which is very important to carry out the mean energy balance peaks at a value of 0.8 at about η = .09 and is slightly higher than what Beuther(1980) measured under stratified conditions. Its shape is close to that of the derivative of the mean derivative Similarly the shear stress uv has a maximum value of about 0.32 at η = 0.07 and is also slightly higher than what Beuther (1980) measured. It should be noted that the shear stress and the radial heat flux have finite values near the center rather than being zero. This is due to the finite values of the various hot-wire error terms for these quantities.

The third and fourth moments are shown in figure (20) through (25). These will be used to balance the transport equations for temperature variance $t^2/2$ and turbulence kinetic energy k. The moments t^2u, u^2t and t^3 all start from a finite value at the center and then show a slight off-axis peak before rolling off. The moment v^3, which represents the radial transport of the radial velocity fluctuations peaks at about η =.07. Again it has a small finite value rather than being zero because of the cross-flow errors. The term vw^2 has a similar shape as v but is smaller in magnitude.

One disappointing feature of the measured third moments is their wide scatter. For the number of samples taken, the relative error for these moments is estimated to be about 10% for a Gaussian signal, which is true in the central region of the plume. This value increases substantially away from the core as the turbulence intensity increases.

4.6 Balances for the Mean Energy and Momentum Equations.

The measured profiles were substituted in the equations of mean momentum and mean energy. The resulting balances are shown in figures (26) and (27) . The error shown is the amount with which one side is smaller or greater than the other. It is seen that these errors are within 10% to 15% of the advection term which are typical for such measurements (c.f. Beuther 1980). It should also be noted that the axial transport and advection terms are almost negligible relative to their radial counterparts. The buoyancy production is almost twice the advection of momentum in the vertical direction which is be expected in flows where buoyancy force is solely responsible for setting up the fluid motion.

It should be noted that these balances help to establish the consistency and accuracy of the experimental data since many of the previous free shear flow experiment are found not to satisfy this constraint.

4.7 Balances for the $t^2/2$ and k Equations

Since the rates of mechanical and thermal dissipation were not measured, the balances equations for the temperature variance $t^2/2$ and turbulence kinetic energy k were evaluated to obtain their values. These balances also help to compare the magnitude of various other terms appearing in these equations.

Since at present there is no method of measuring the pressure diffusion terms it was decided to make an estimate of these. For this purpose we used the second order closure scheme of Lumley (1978) which gives

$$\overline{pu_i} = - \overline{q^2 u_i} / 5 \qquad (4.8)$$

i.e the pressure transport in a given direction is about 20% of the turbulent transport in that direction. It is realized that there is no experimental verification of the above relation, but at the same time is believed that it is better to use this estimate rather than just setting the pressure diffusion equal to zero. This also means that the term labelled ''disspation'' in following graphs is really the sum of the dissipation, the errors due to the above assumption and the measurement errors present in the other terms. If the correction for the pressure diffusion term were not included, the ''dissipation'' terms would be smaller by approximately 8%.

The equations for the temperature variance and turbulence kinetic energy are given in section 2.5

Figures (28) and (29) show the balances for these equations. At the centerline the buoyancy production of turbulence energy is about 60% of the advection terms. After about η = 0.08 the advection term becomes negative, implying that at the outer edges the kinetic energy is being advected downwards. Also the axial transport of kinetic energy by the turbulence is very small as compared to the radial.

It should be mentioned that little confidence can be placed in these balances beyond η =.1 or so due to the various measurement errors associated with flow reversals and cross-flow on hot wires.

6. CONCLUSIONS

The velocity and thermal fields were measured in a turbulent buoyant plume in a neutral environment using two wire and three wire probes. From the digitally recorded velocity and temperature signals, various moments were calculated upto fourth order. Source conditions

were carefully monitored to calculate the source buoyancy which for an ideal gas in a neutral environment must remain constant. Thermocouples, placed at various heights, were used to measure the ambient temperature in order to make sure that the ambient was not stratified. Also an array of sixteen thermocouples was used to establish the axisymmetry of the flow. The results of the experiments are summarized below.

1. The following mean buoyancy and temperature profiles are recommended for an axisymmetric turbulent buoyant plume:

$$t = 9.4/[1+28\eta^2]^2 \quad \text{or} \quad 9.4 \exp [- 69\eta^2]$$

and

$$f = 3.2/[1+28\eta^2]^2 \quad \text{or} \quad 3.2 \exp [- 57\eta^2]$$

The exponential forms are to be preferred for integration, and especially for the volume flow rate.

2. The centerline turbulent intensities of temperature and velocity were 40% and 33% respectively, and the temperature-vertical velocity correlation coefficient was about 0.68. These are in excellent agreement with the results of George et al (1977).

3. The experiment satisfies both the integral and the differential forms of the mean momentum and energy equations for a neutral environment, thus giving confidence to the measurements.

4. The rates of mechanical and thermal dissipation were

obtained as the closing entries in balances of the turbulence kinetic energy and the temperature variances. The pressure transport appearing in the kinetic energy was not measured and was approximated with a formula due to Lumley (1978). Because of various measurement errors these balances should be interpreted carefully beyond $\eta = 0.1$.

REFERENCES

Baker, C.B. (1980) An Analysis of the Turbulent Buoyant Jet. PhD Dissertation, SUNY at Buffalo, Buffalo, NY.

Batchelor, G.K. (1954) Heat Convection and Buoyancy Effects in Fluids. Quart. J. Royal Met. Soc. V.80, p. 339.

Beuther, P.D. (1980) An Experimental Investigation of the Turbulent Buoyant Plume. PhD Dissertation, SUNY at Buffalo, Buffalo, NY

Beuther, P.B. and George, W.K., (1982) The Turbulent Buoyant Plume in a Stratified Environment. Proc. of Nat. Cong. Theor. and Appl. Mech., Cornell Univ., Ithaca, NY

Champagne, F.H. and Sleicher, C.A. (1967) Turbulence Measurements with Inclined Wires. Part I, J. Fluid Mech. 28, 177.

George, W.K., Jr., Alpert, R.L., Tamanini, F. (1977) Turbulence Measurements in an Axisymmetric Buoyant Plume. Int. J. Heat Mass Trans. V.20, 1145-1154.

George, W.K., Beuther, P.B. and Shabbir, A. (1987) X-wire Response in Turbulent Flows of High Intensity Turbulence and Low Mean Velocities. Symp. on Thermal Anemometry, Cincinnati, OH.

George, W.K., Beuther, P.D., and Shabbir, A. (1987) Polynomial Calibrations for Hot Wires in Thermally-Varying Flows. Symp. on Thermal Anemometry, Cincinnati, OH.

George, W.K. and Shabbir, A. (1987) The Effect of Screens and Co-flow on Turbulent Buoyant Plumes. To be submitted.

Hossain, M.S. and Rodi, W. (1982) A Turbulence Model for Buoyant Flows and Its Application to Buoyant Jets. Turbulent Buoyant Jets and Plumes, ed. W. Rodi, Pergamon, NY, p. 121-178.

Kotsovinos, N.E. (1977) Plane Turbulent Buoyant Jets, Part 1, J. Fluid Mech. 81, p. 1 part 2, p. 45.

Launder, B.E. (1975) On the Effects of a Gravitational Field on the Turbulent Transport of Heat and Momentum. J. Fluid Mech. V. 67, pp. 569-590.

Lumley, J.L. (1978) Computational Modeling of Turbulent Flows. Advances in Applied Mechanics, V. 18, pp. 123-176.

Lumley, J.L., Zeman, O. and Siess, J. (1978) The Influence of Buoyancy on Turbulent Transport. J. Fluid Mech., 84, Pt.3, O. 581.

List, E.J. and Imberger, J. (1973) Turbulent Entrainment in Buoyant Jets and Plumes. Proc. ASCE, J. Hyd. Div., 99, p.1416-1474.

Morton, B.R. (1959) Forced Plumes. J. Fluid Mech.,2, p.151-163.

Morton, B.R., Taylor, G.I. and Turner, J.S. (1956) Turbulent Gravitational Correction from Maintained and Instantaneous Sources. Proc. Roy. Soc. A234, p. 1-23.

Nakagome, H. and Hirata, M. (1977) The Structure of Turbulent Diffusion in an Axi-symnmetrical Thermal Plume. Heat Trans. & Turbulent Buoyant Convection, (Spalding and Afgan, eds.) McGraw-Hill, NY 367-372.

Rouse, J., Yih, C.S. and Humphrey, H.W. (1952) Gravitational Convection from a Boundary Source. Tellus, 4, p. 201-10.

Schmidt, W. (1941) Turbulent Propagation of a Stream of Air. ZAMM, V21 6.

Tennekes, H. and Lumley, J.L. (1972) A First Course in Turbulence, MIT Press.

Tutu, N.K. and Chevray, R. (1975) Cross-wire Anemometry in High Intensity Turbulence, J. Fluid Mech., 71, p. 785.

Webster, C.A.G. (1962) J. Fluid Mech. 13, p. 307.

Zel'dovich, Ya B. (1937) Limiting Laws for Turbulent Flows in Free Convection, Zh. EKSP. Teoret. Fiz. 7(12), 1463.

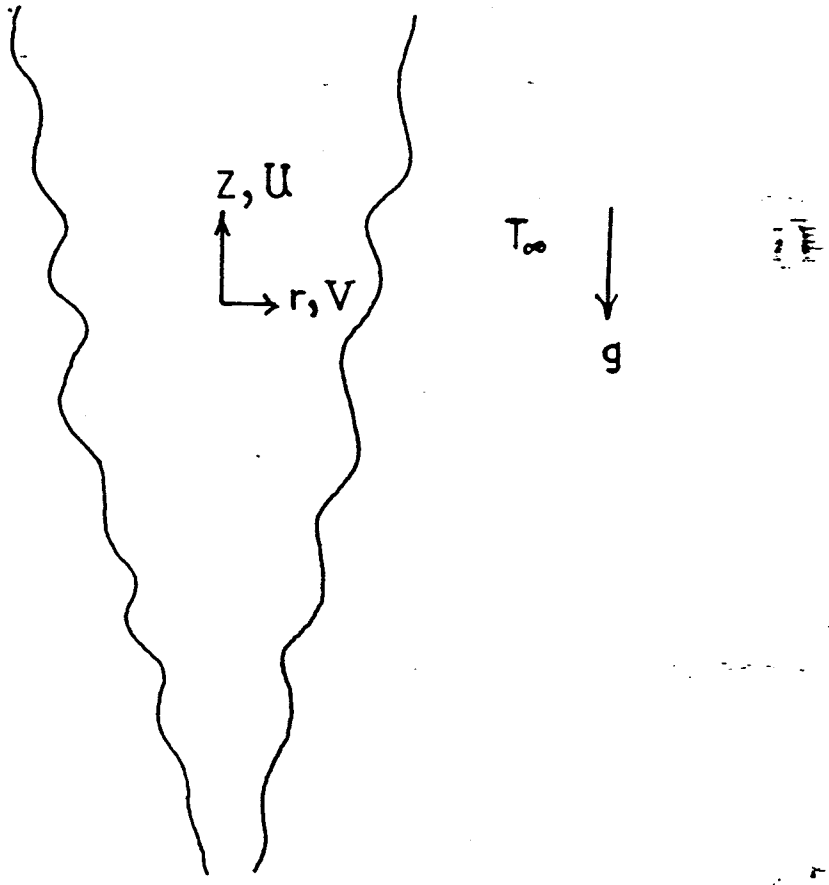

FIGURE 1

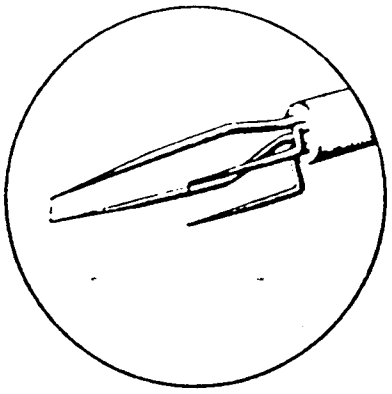

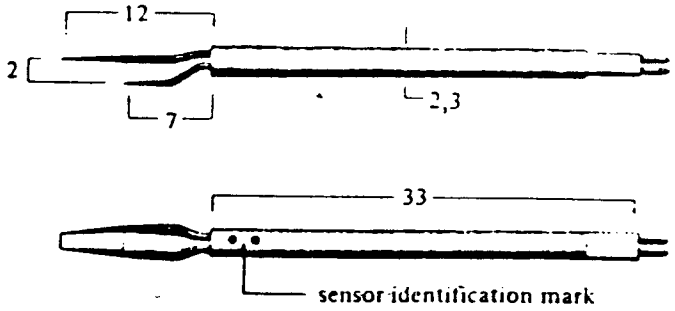

55P76

Straight type, velocity sensor perpendicular to probe axis, for velocity measurements at fluctuating medium temperatures.

Velocity sensor is Pt-plated tungsten wire, diameter 5 µm, overall length 3 mm, sensitive wire length 1.25 mm. Copper and gold plated at the ends to a diameter of approx. 30 µm

(a)

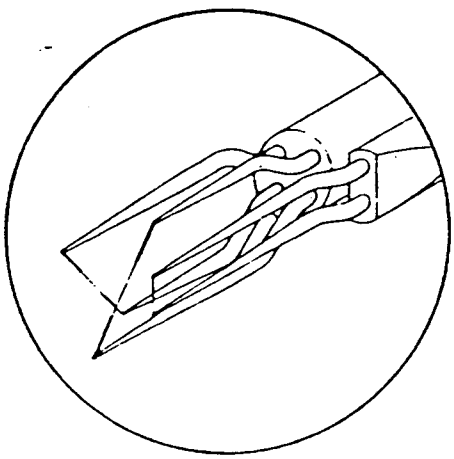

X-probe with Temperature Sensor

Standard X-array with additional temperature sensor for 2-dimensional work. Velocity sensors are 5 µm gold-plated tungsten wires and temperature sensor is 1 µm platinum wire. Spatial resolution approximately 2 mm.

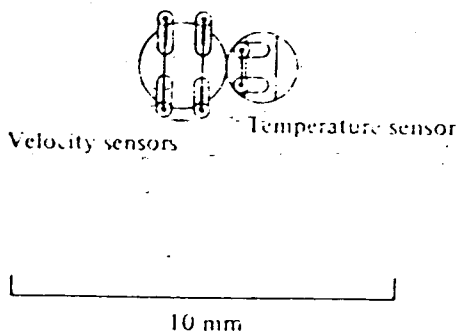

(b)

FIGURE 2

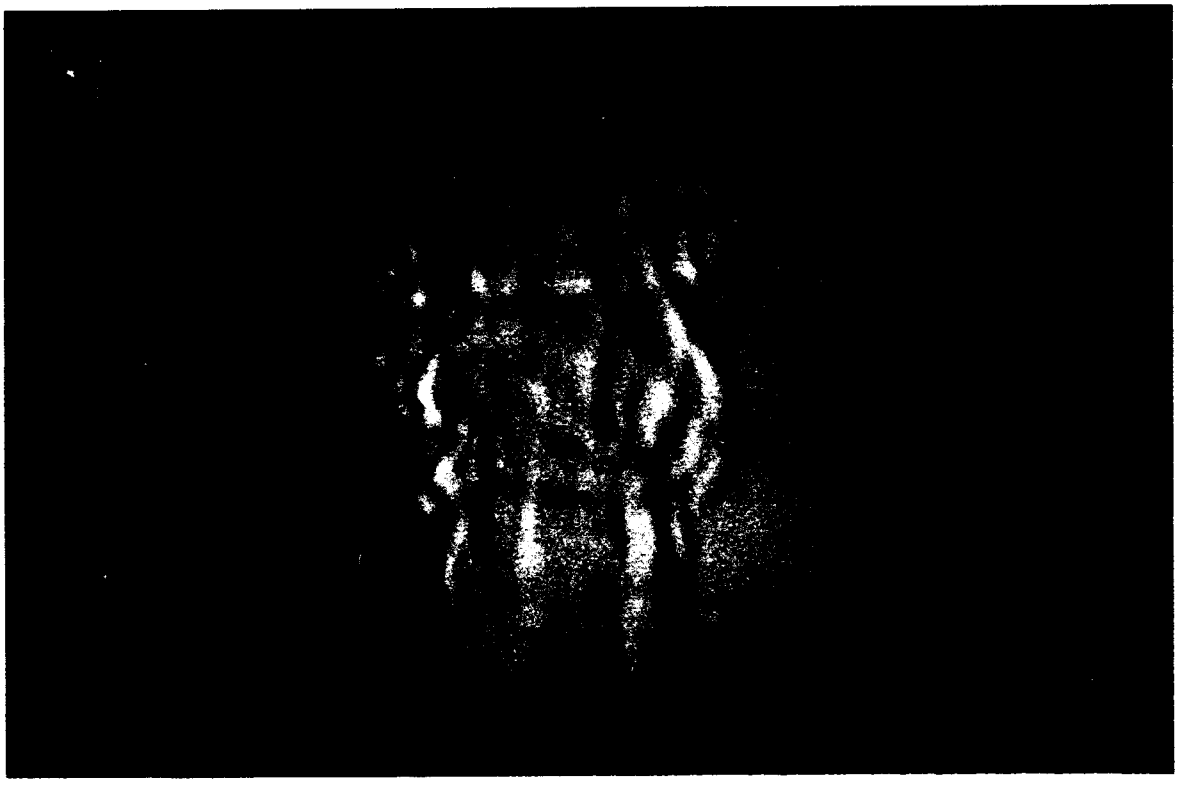

FIGURE ~~12~~ 3

TABLE I

EXPT.	T_0 (°C)	U_0 (m/s)	F_0 (m^4/s^3)	M_0 (m^4/s^2)
SINGLE WIRE	295	0.98	0.0127	0.0030
X-WIRE	295	0.86	0.0115	0.0023

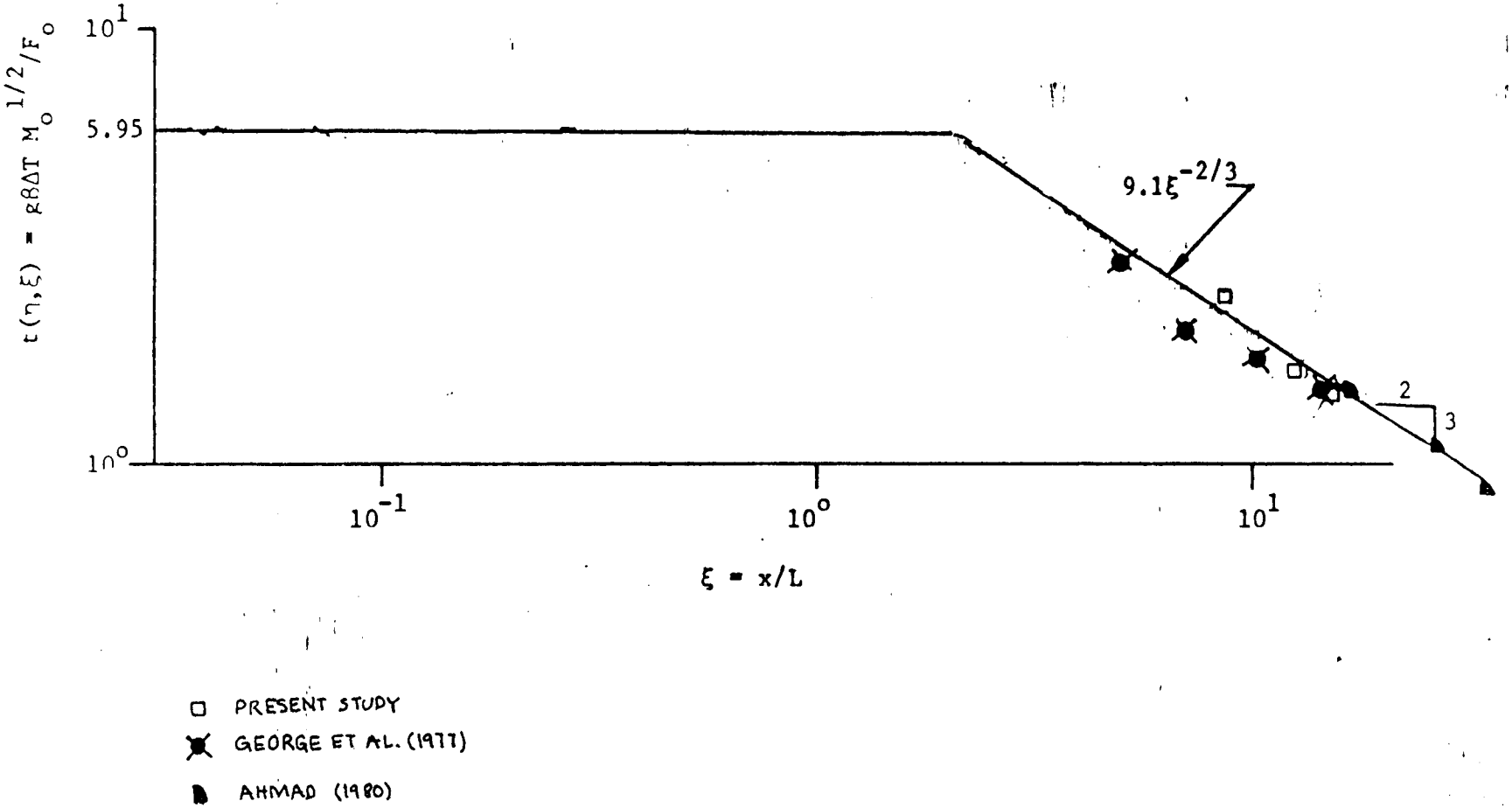
10^1
5.95
10^0
$\xi(\eta,\xi) = \rho\beta\Delta T\, M_o^{1/2}/F_o$
$9.1\xi^{-2/3}$
2
3
10^{-1}
10^0
10^1
$\xi = x/L$
PRESENT STUDY
GEORGE ET AL. (1977)
AHMAD (1980)

FIGURE 4

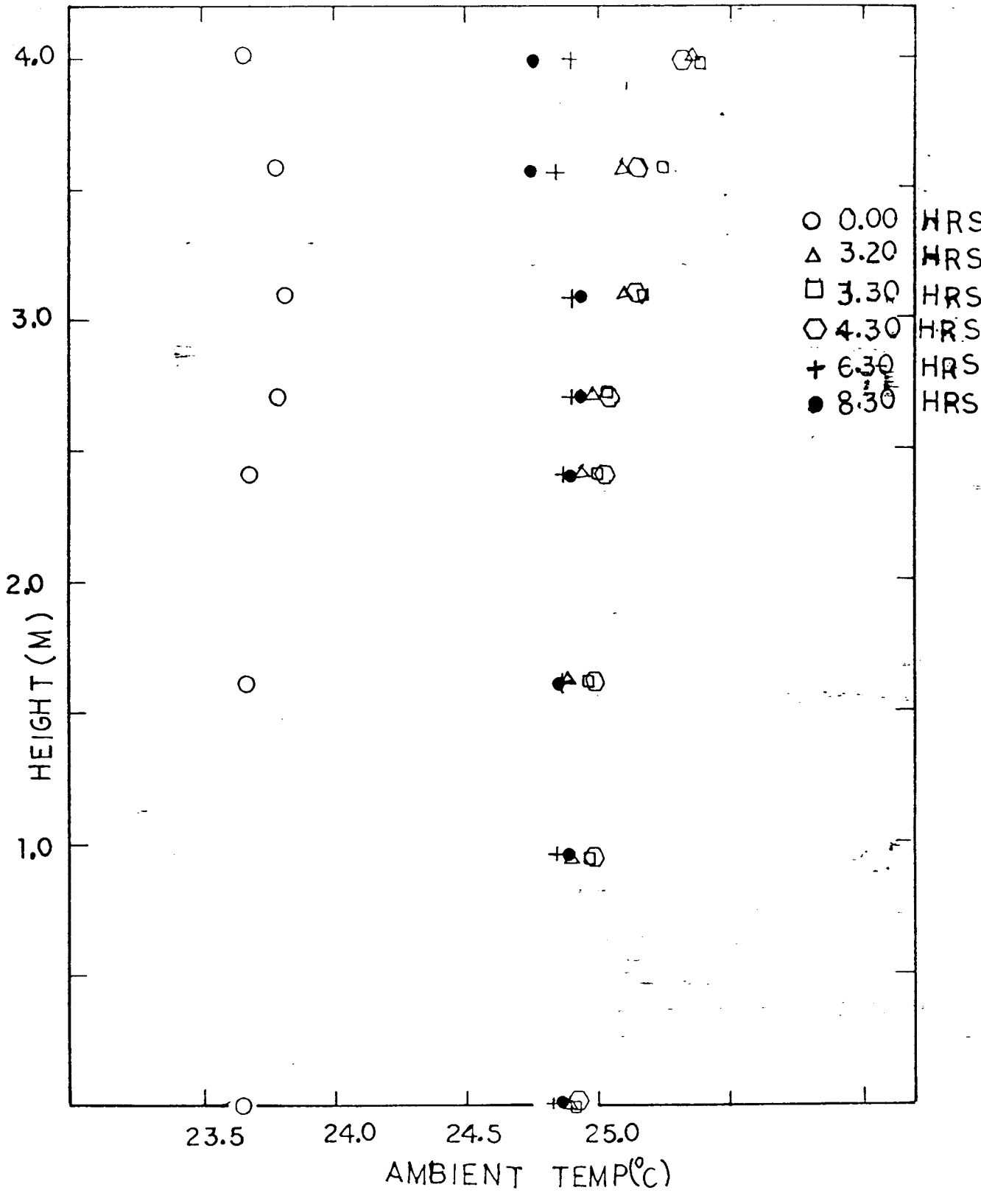
4.0
3.0
2.0
1.0
HEIGHT (M)
23.5
24.0
24.5
25.0
AMBIENT TEMP(°C)
0.00 HRS
3.20 HRS
3.30 HRS
4.30 HRS
6.30 HRS
8.30 HRS

FIGURE ~~14~~ 5

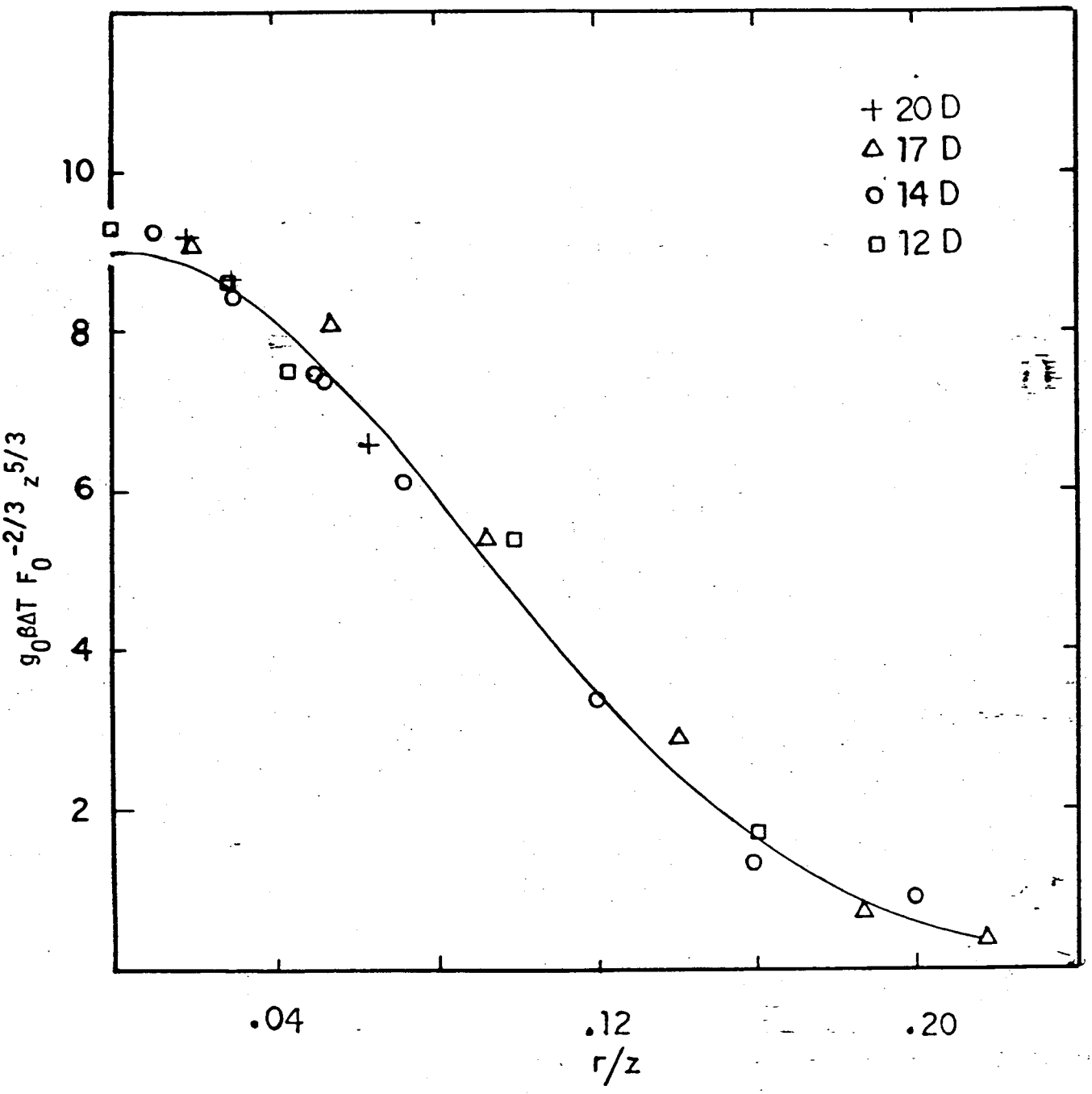

FIGURE 22 6

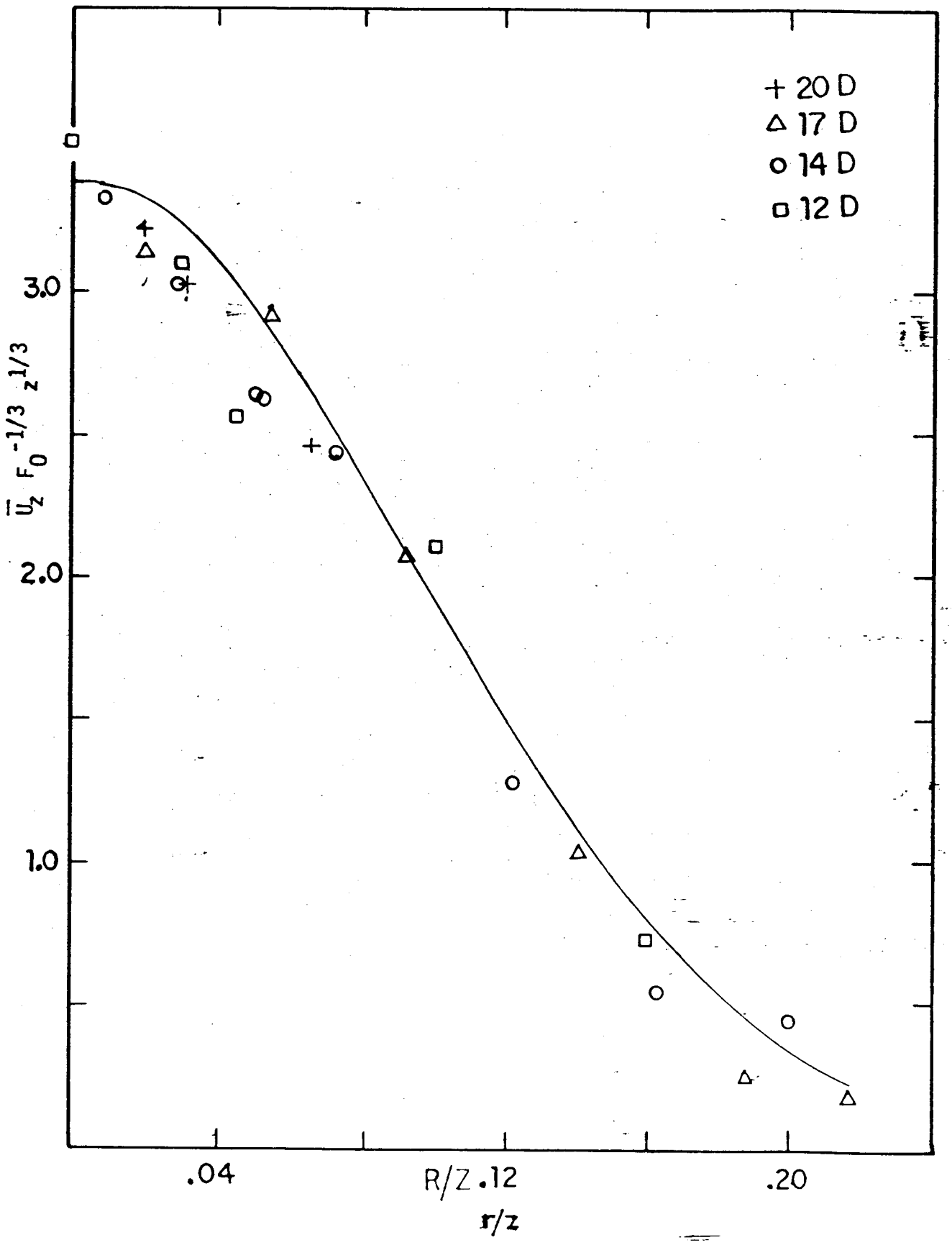
+ 20 D
△ 17 D
o 14 D
□ 12 D
3.0
2.0
1.0
$\bar{U}_z F_0^{-1/3} z^{1/3}$
.04
R/Z .12
.20
r/z

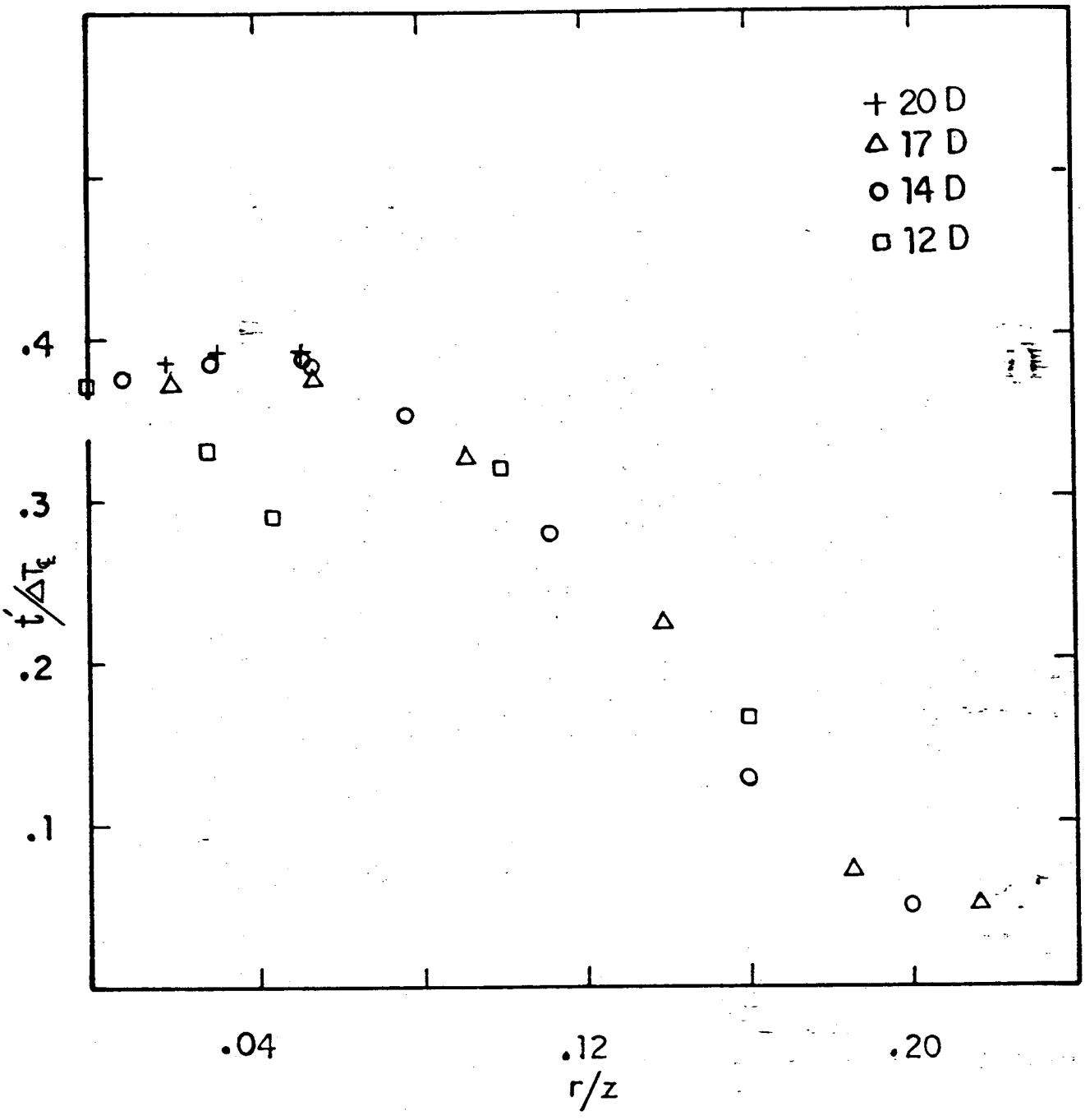

FIGURE ~~24~~ 8

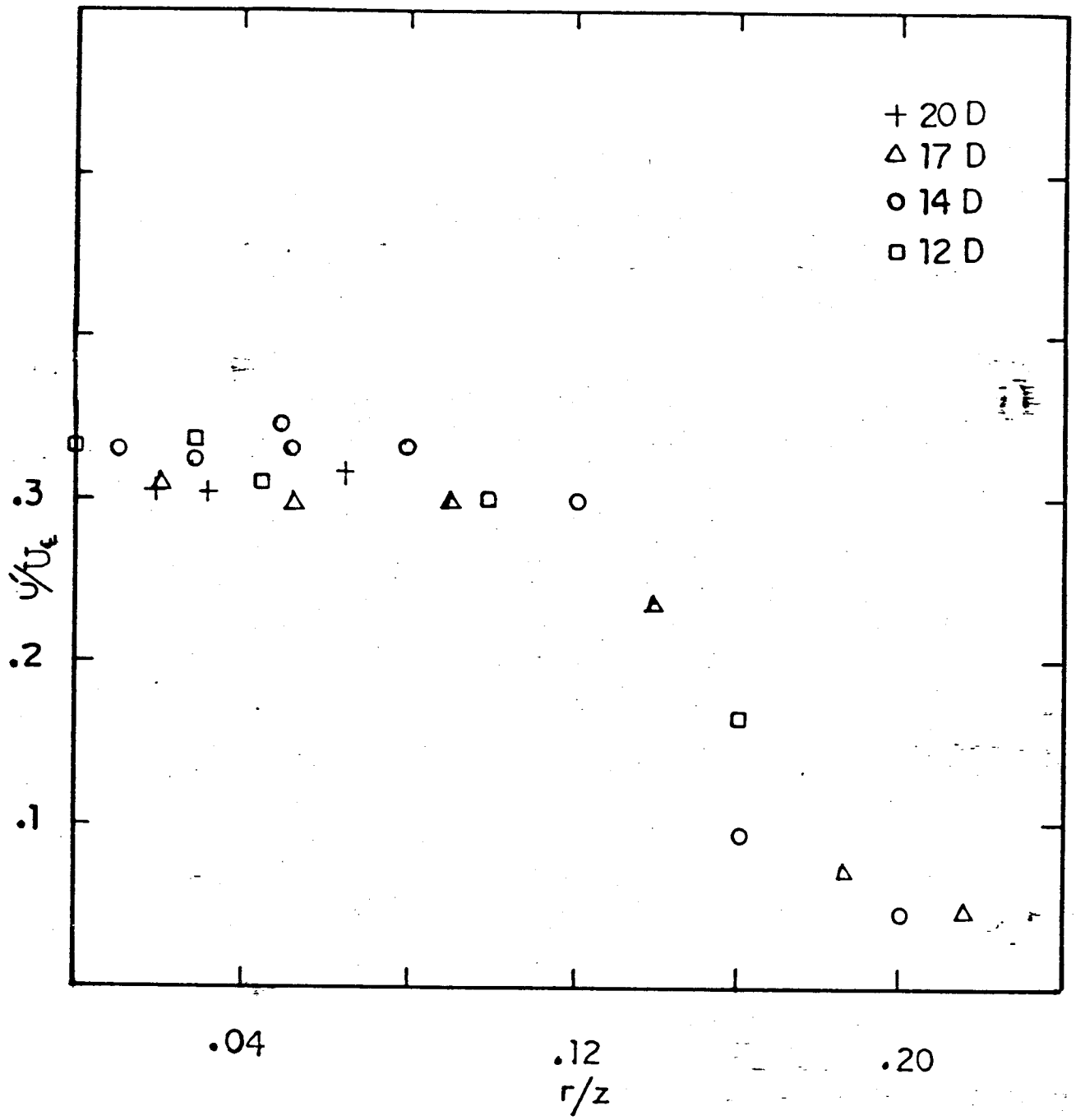

FIGURE 25 9

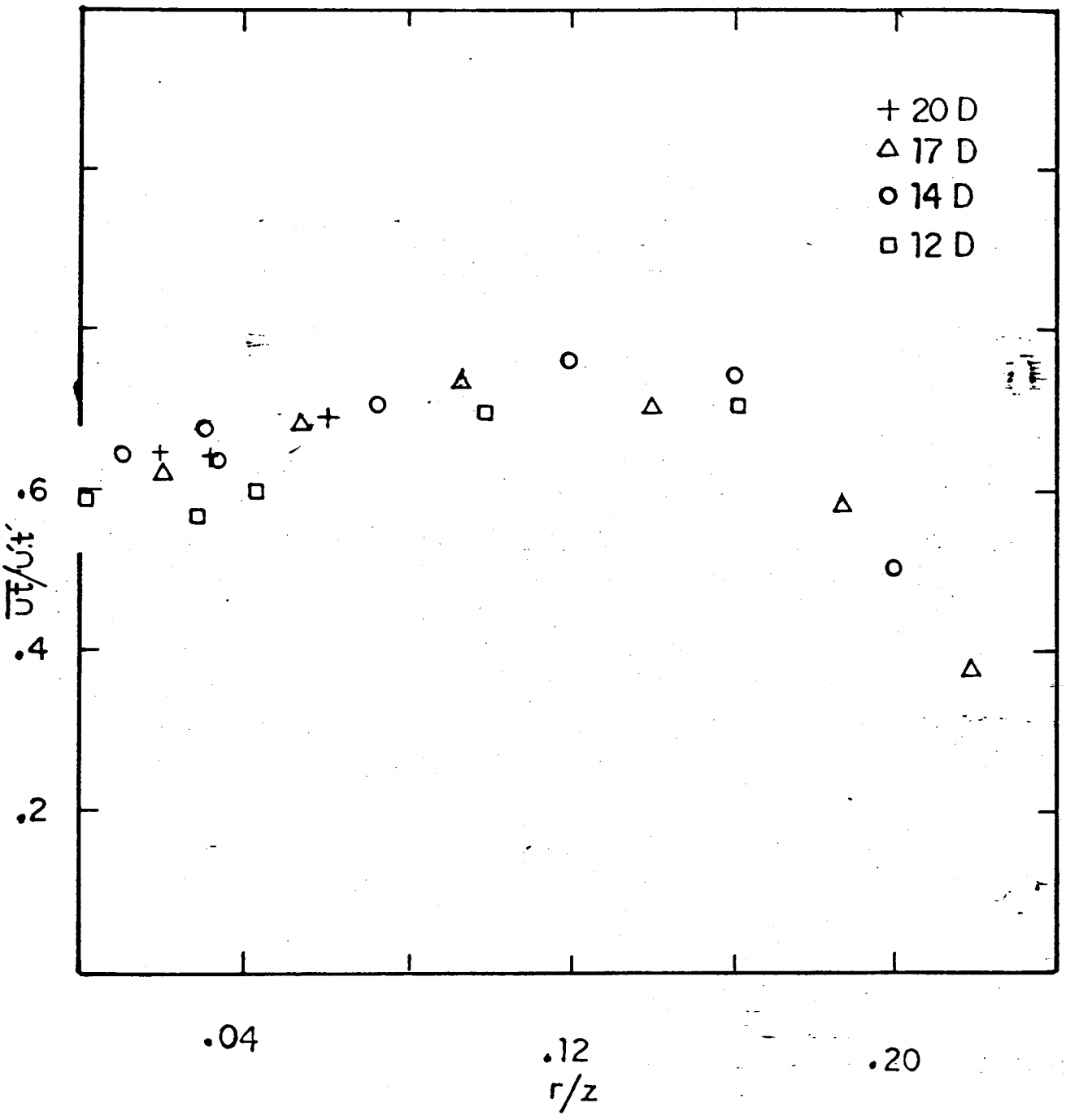

FIGURE ~~26~~ 10

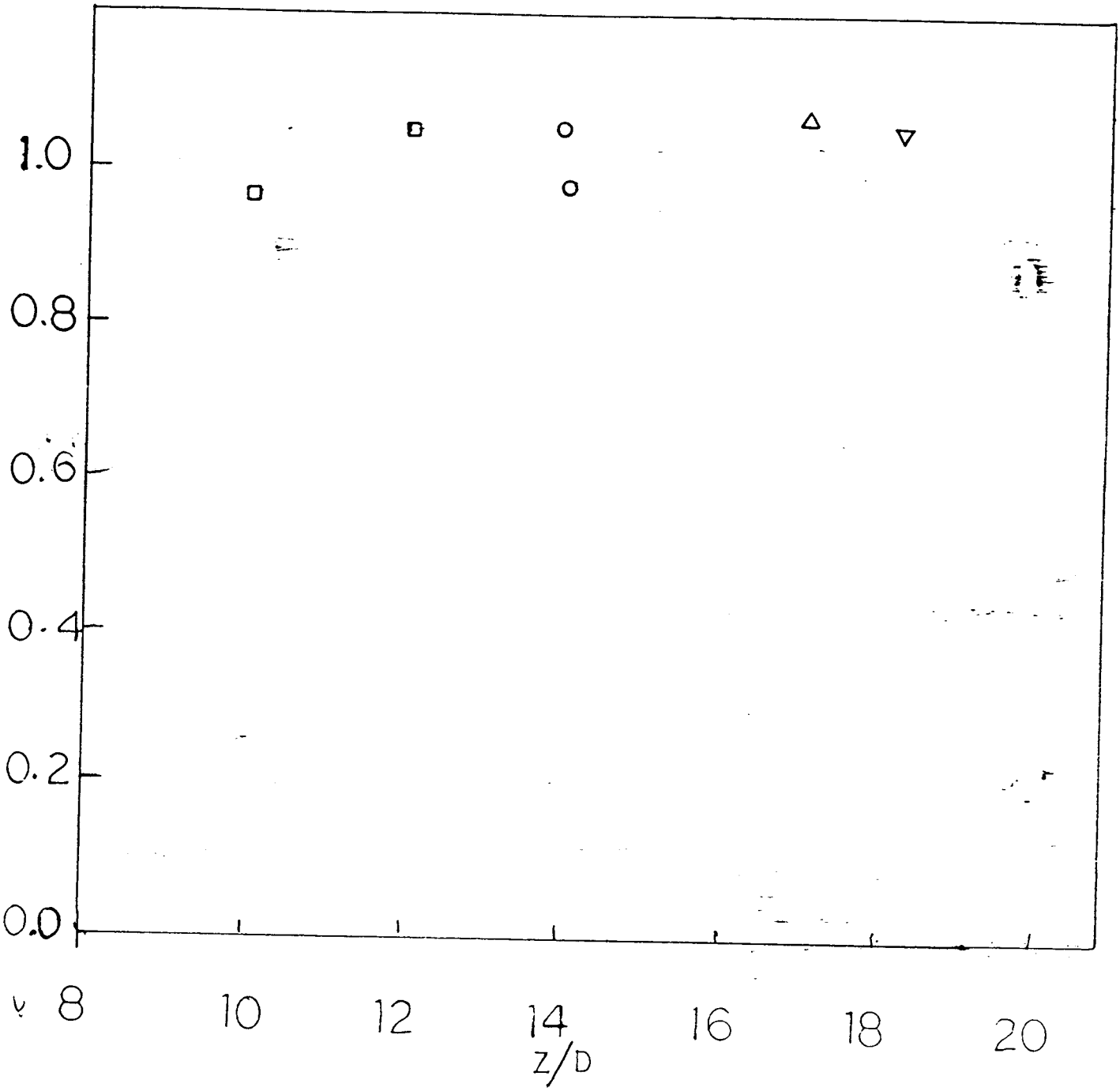

FIGURE 26 a

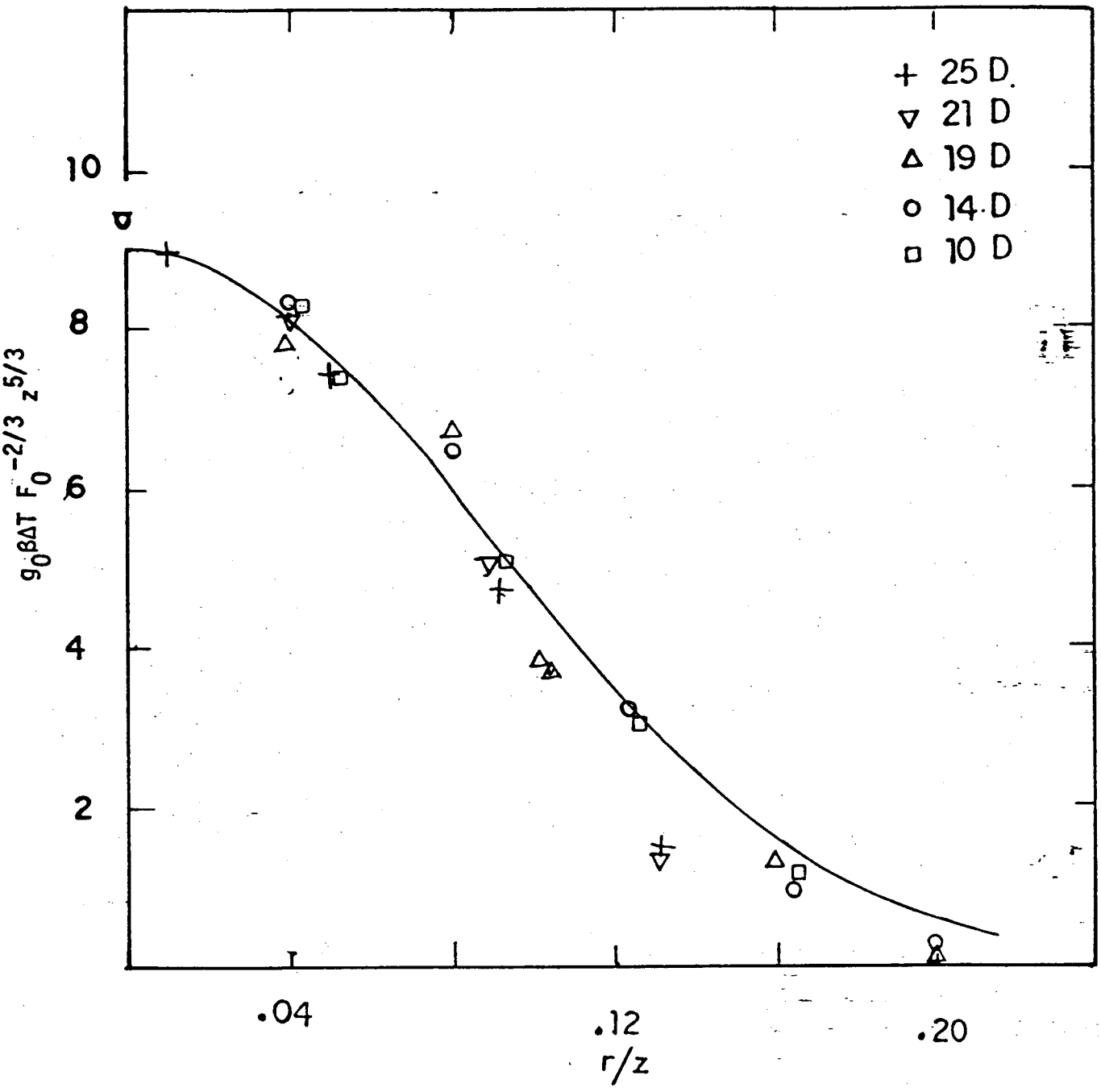

FIGURE ~~27~~ 12

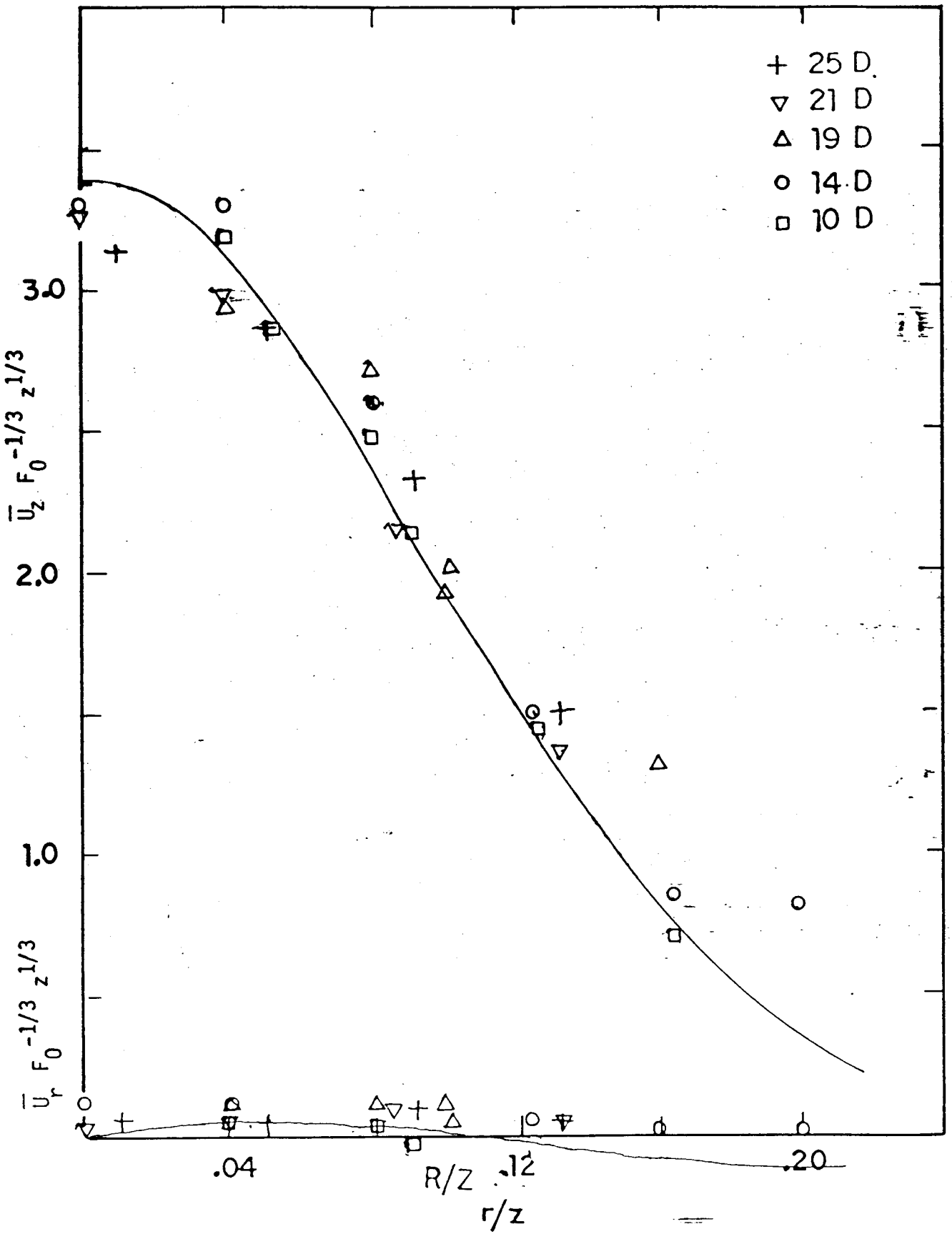
+ 25 D
▽ 21 D
△ 19 D
o 14 D
□ 10 D
3.0
2.0
1.0
$\bar{U}_z F_0^{-1/3} z^{1/3}$
$\bar{U}_r F_0^{-1/3} z^{1/3}$
.04
.12
.20
R/Z
r/z

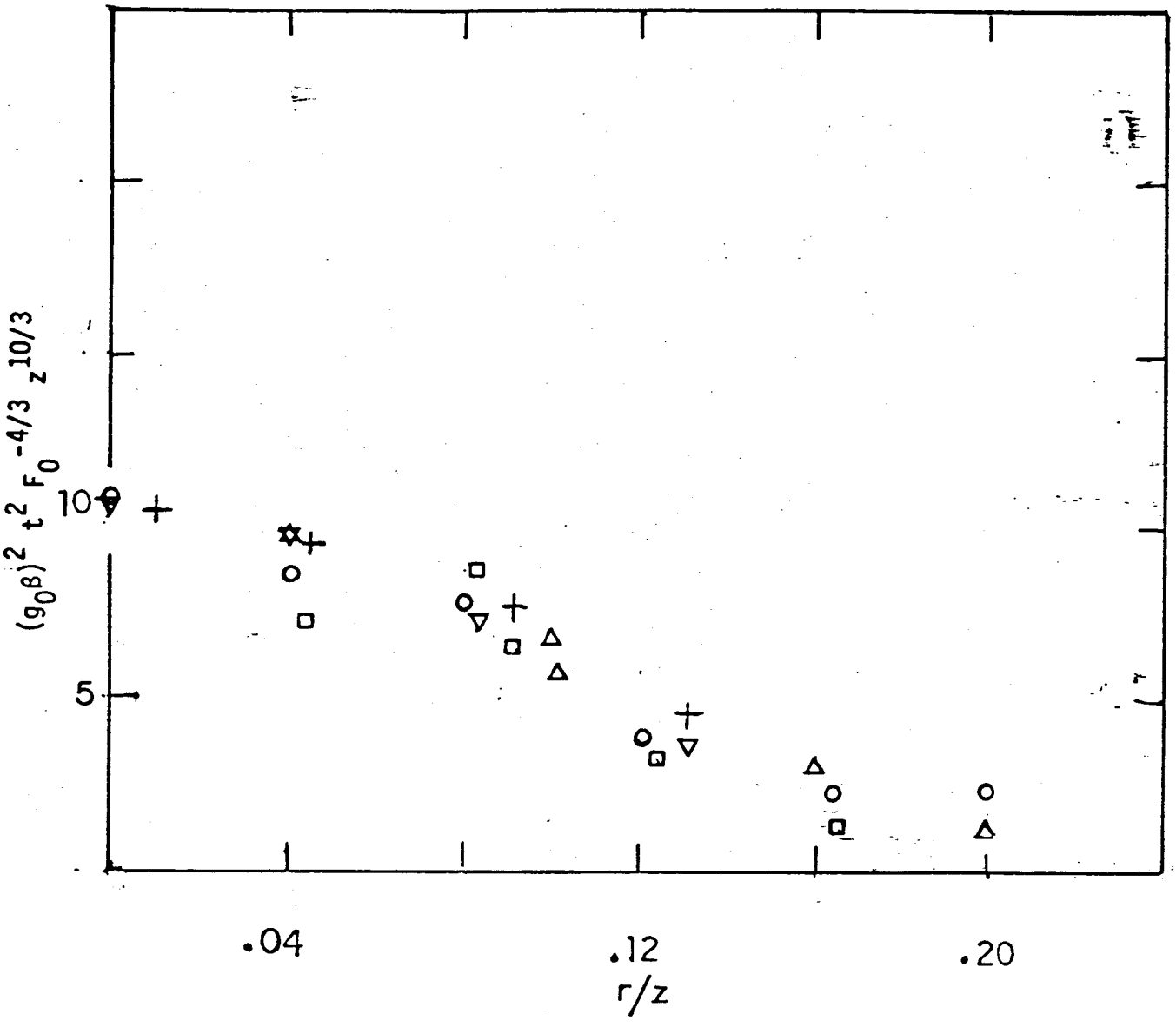

FIGURE ~~29~~ 14

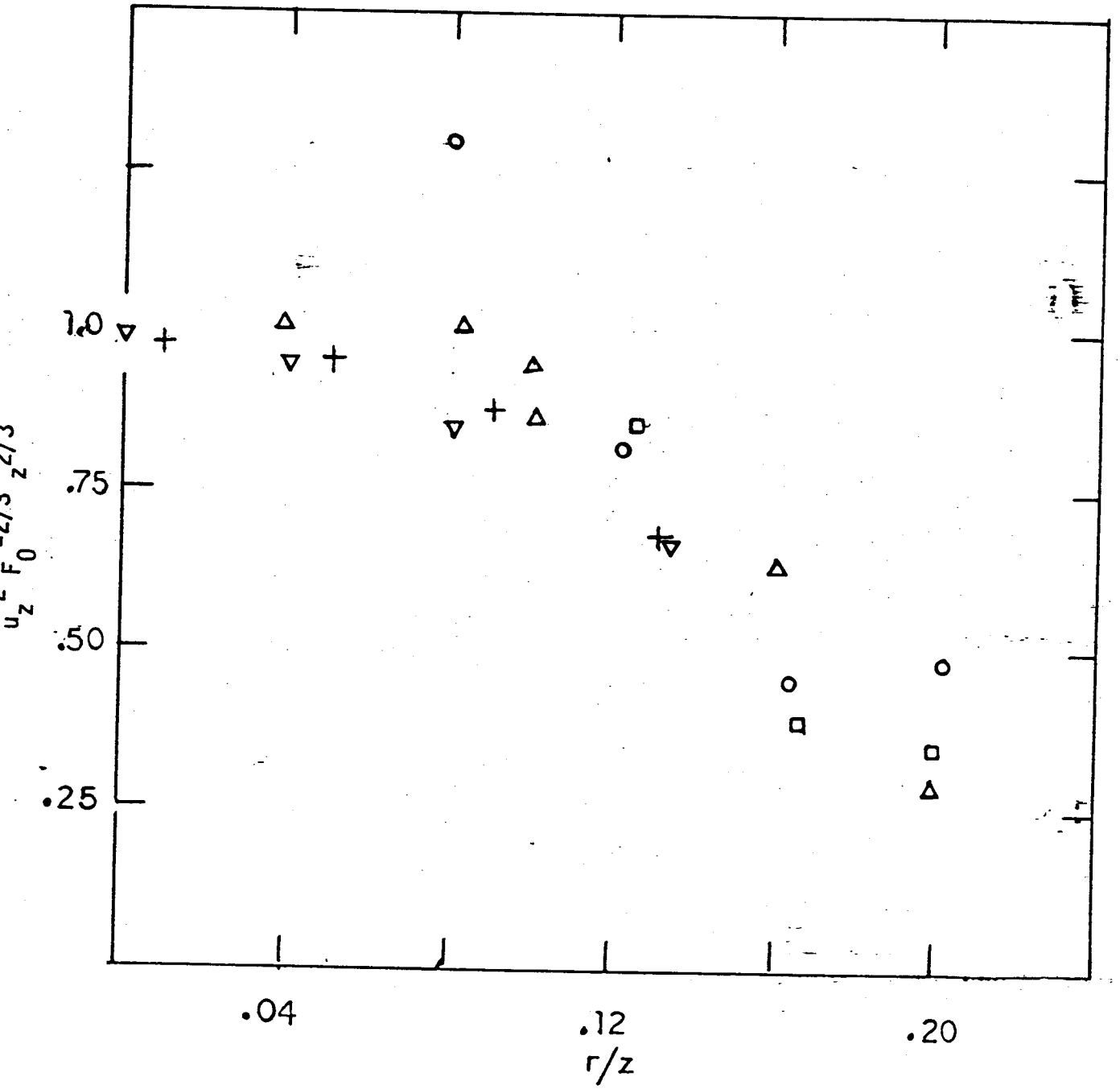

FIGURE ~~30~~ 15

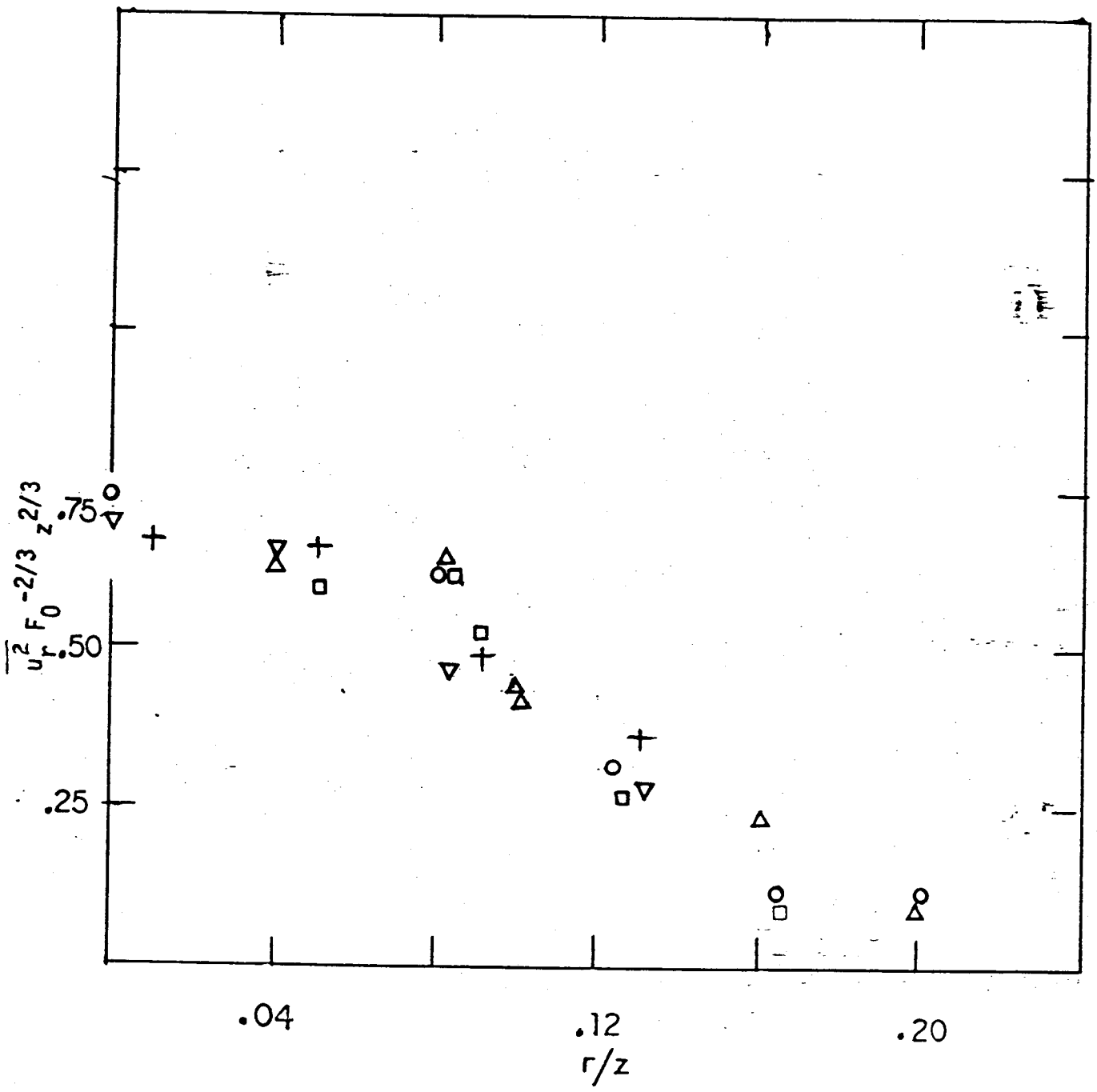

FIGURE 31 16

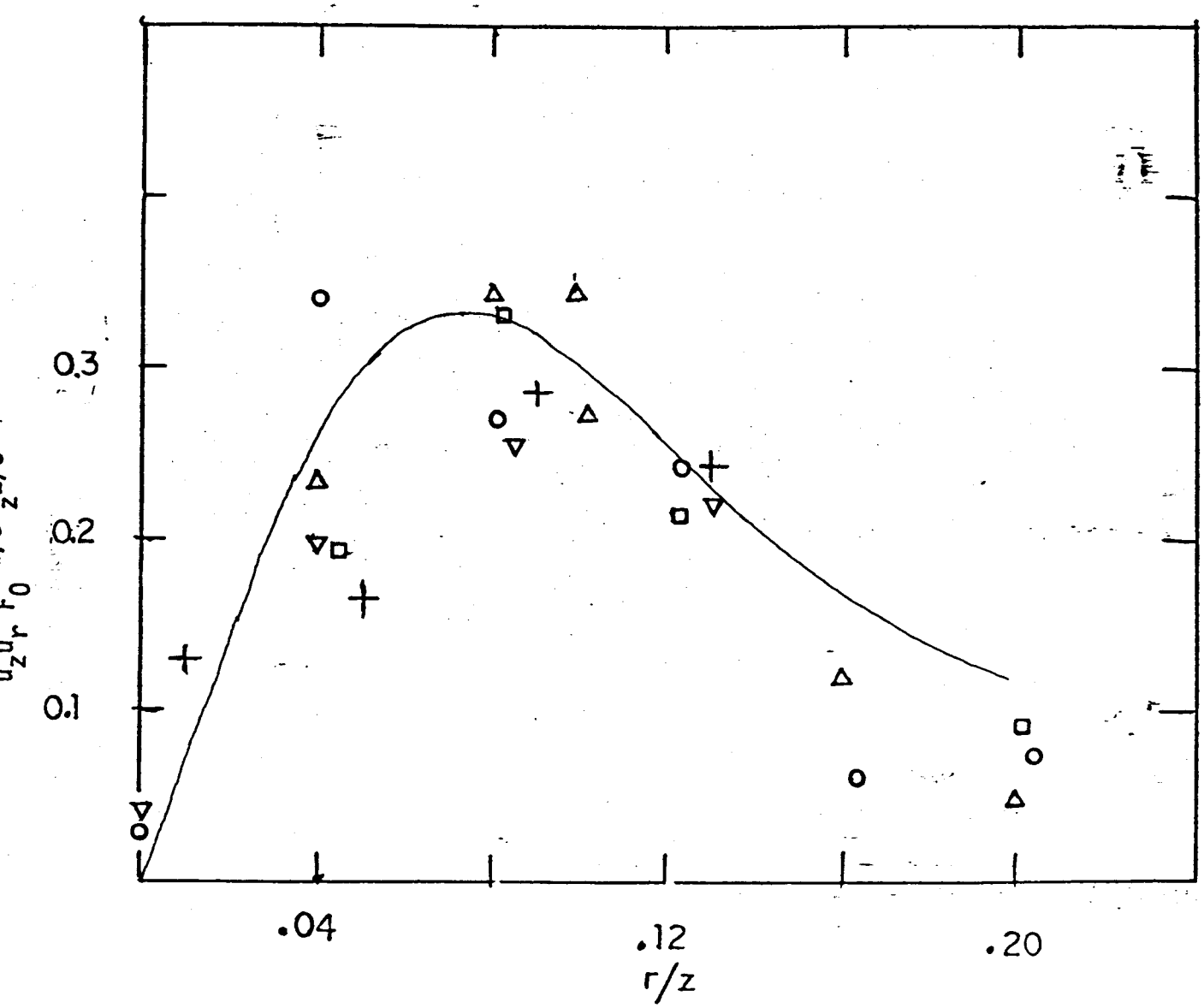

FIGURE ~~32~~ 17

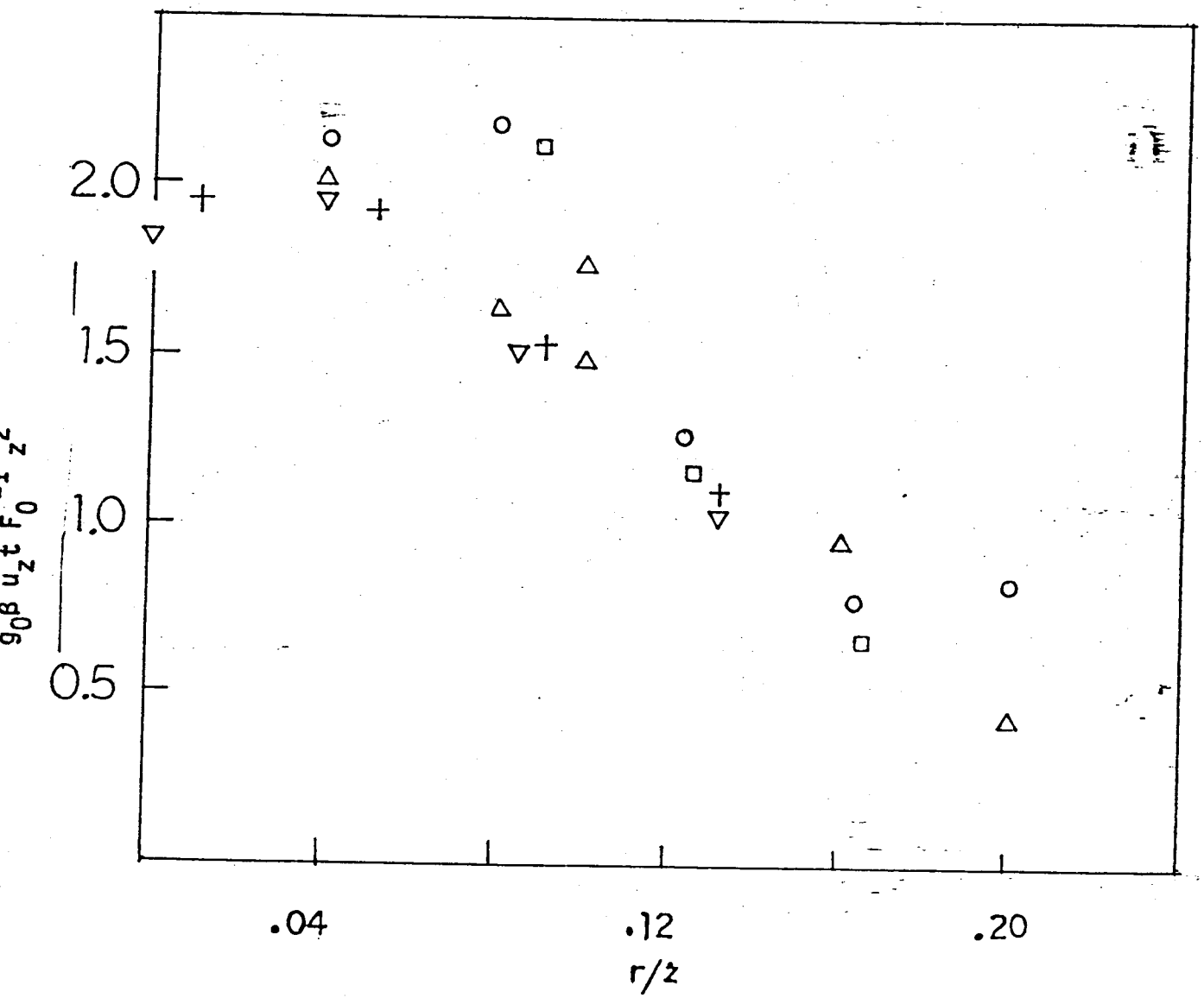

FIGURE ~~33~~ 18

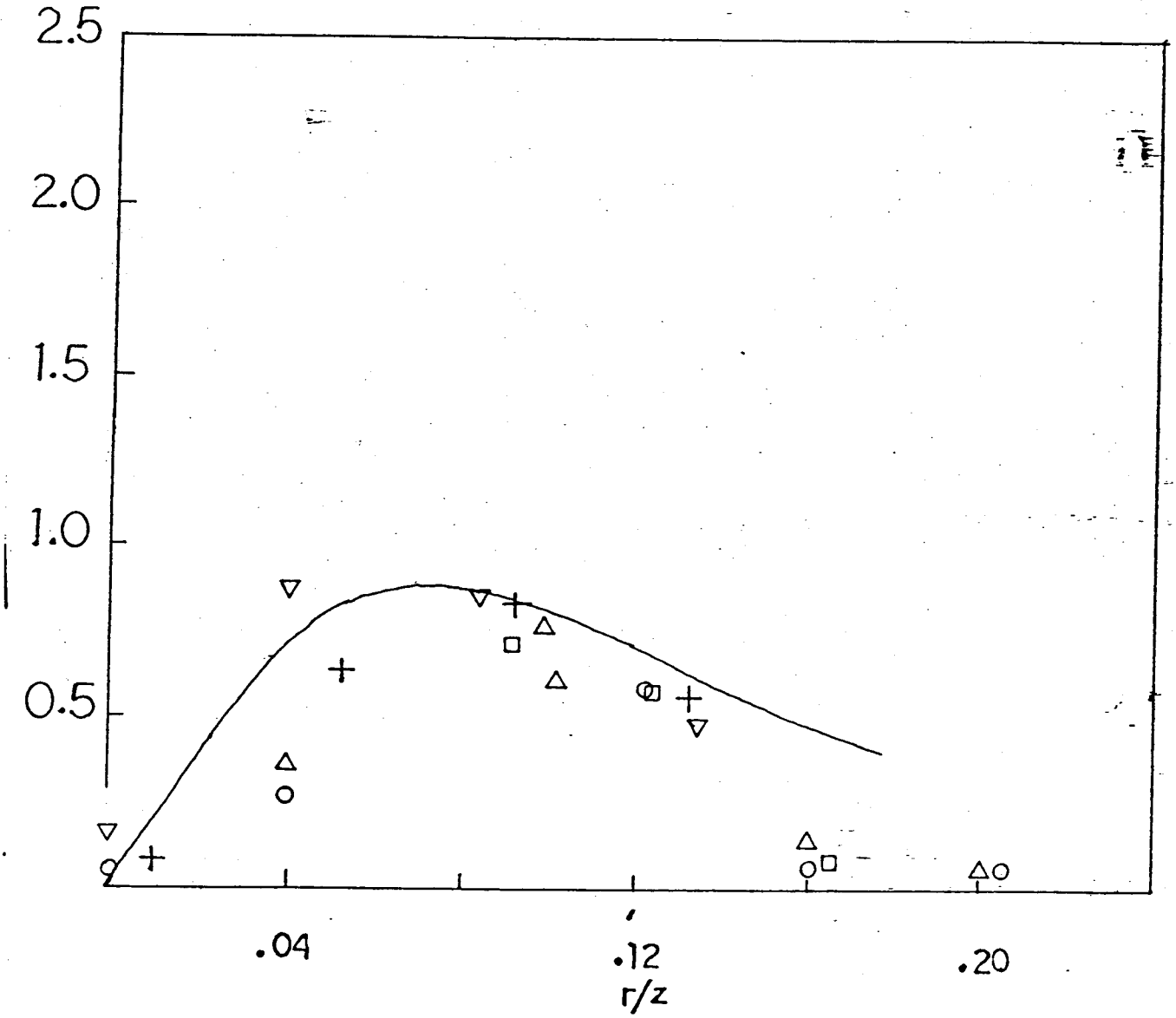

FIGURE 34

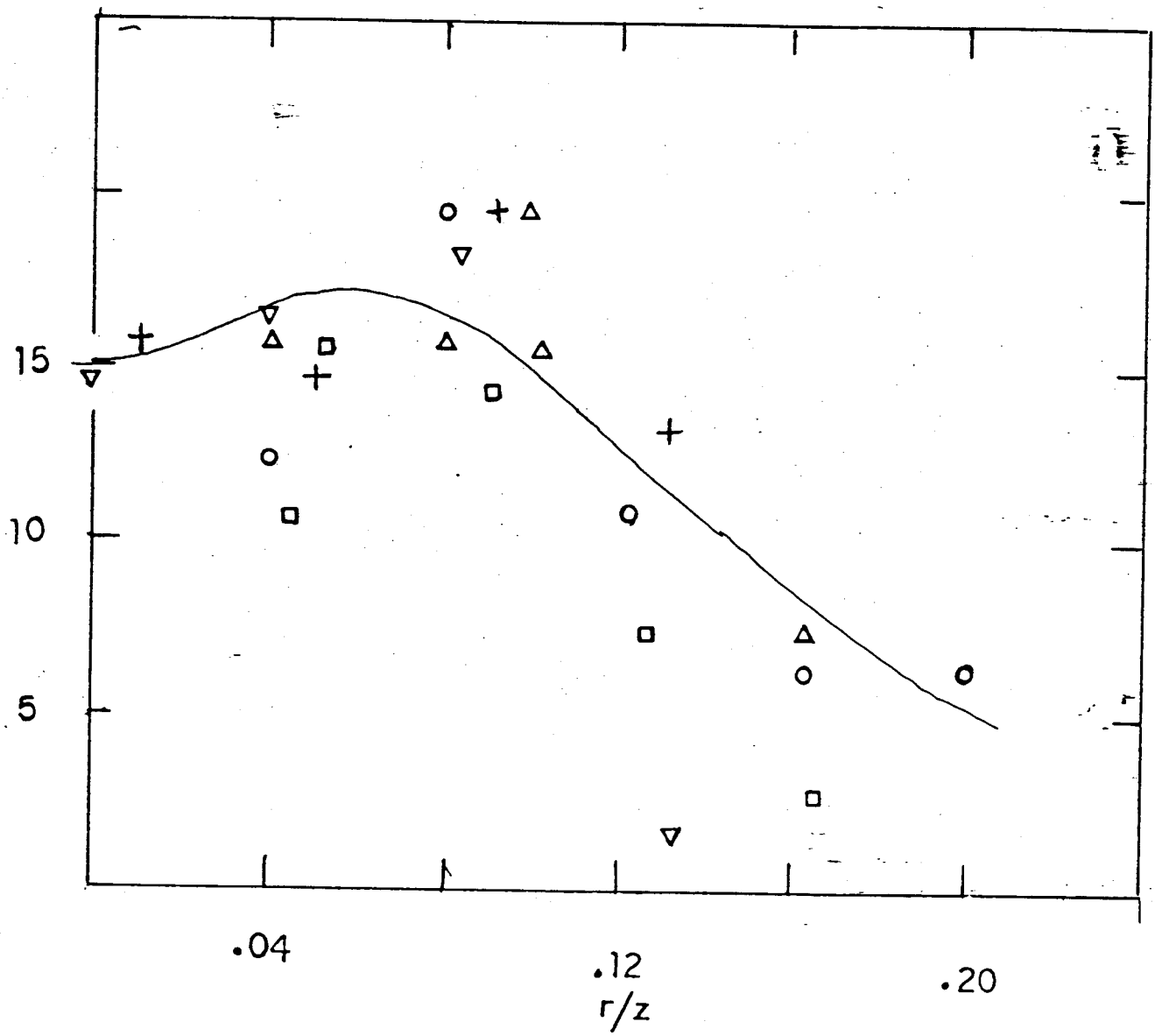

FIGURE ~~35~~ 20

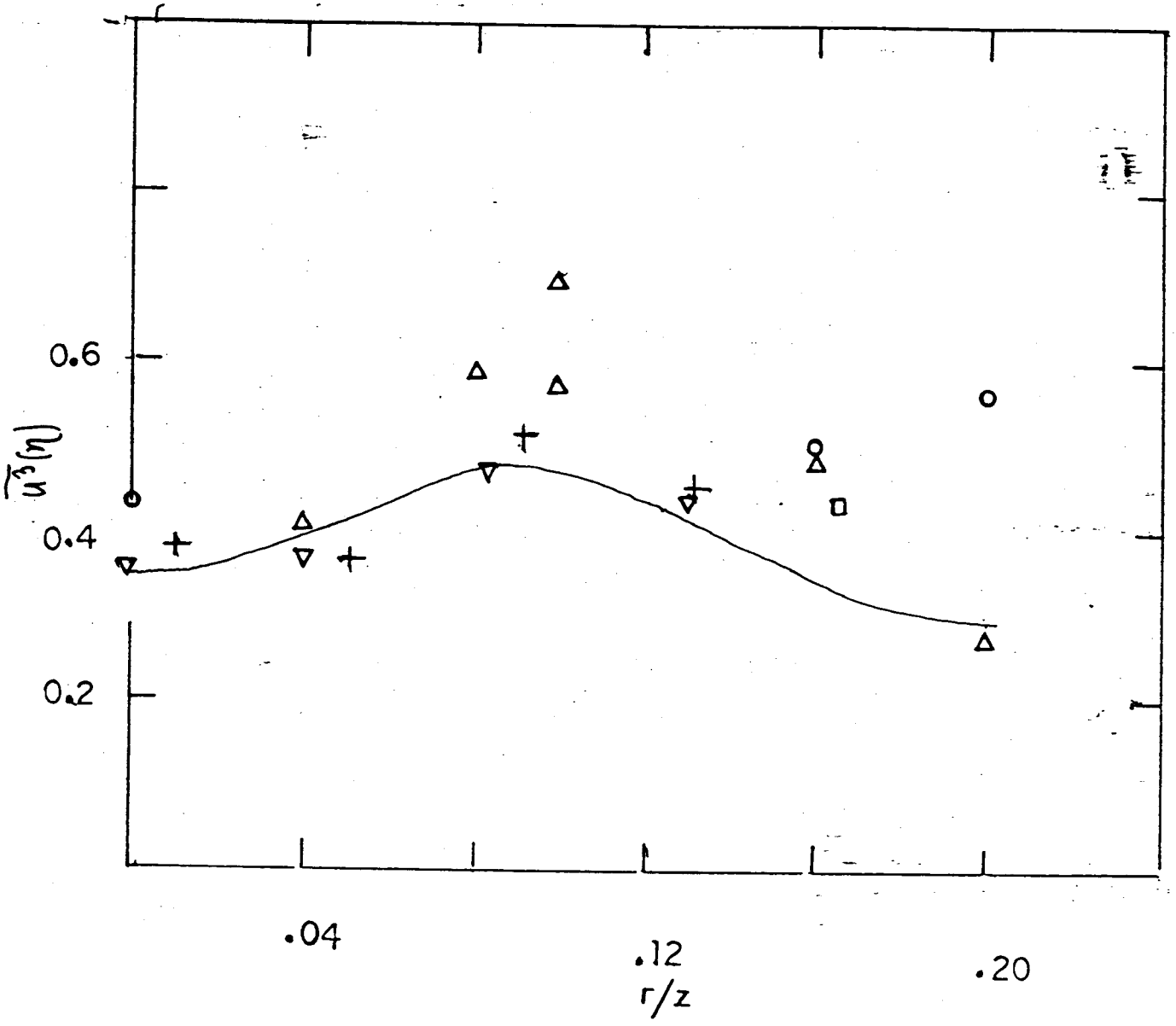

FIGURE 36 21

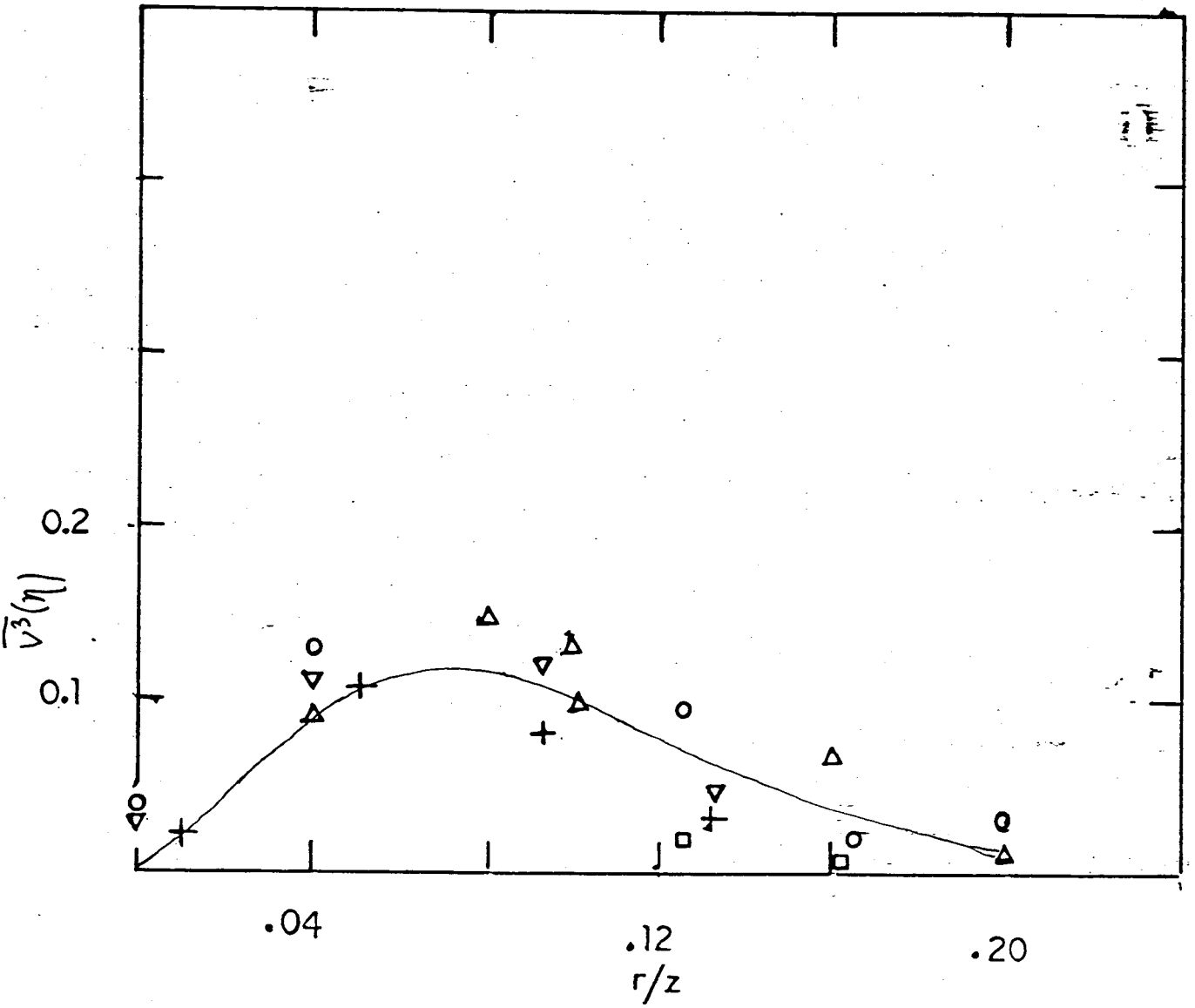

FIGURE 37

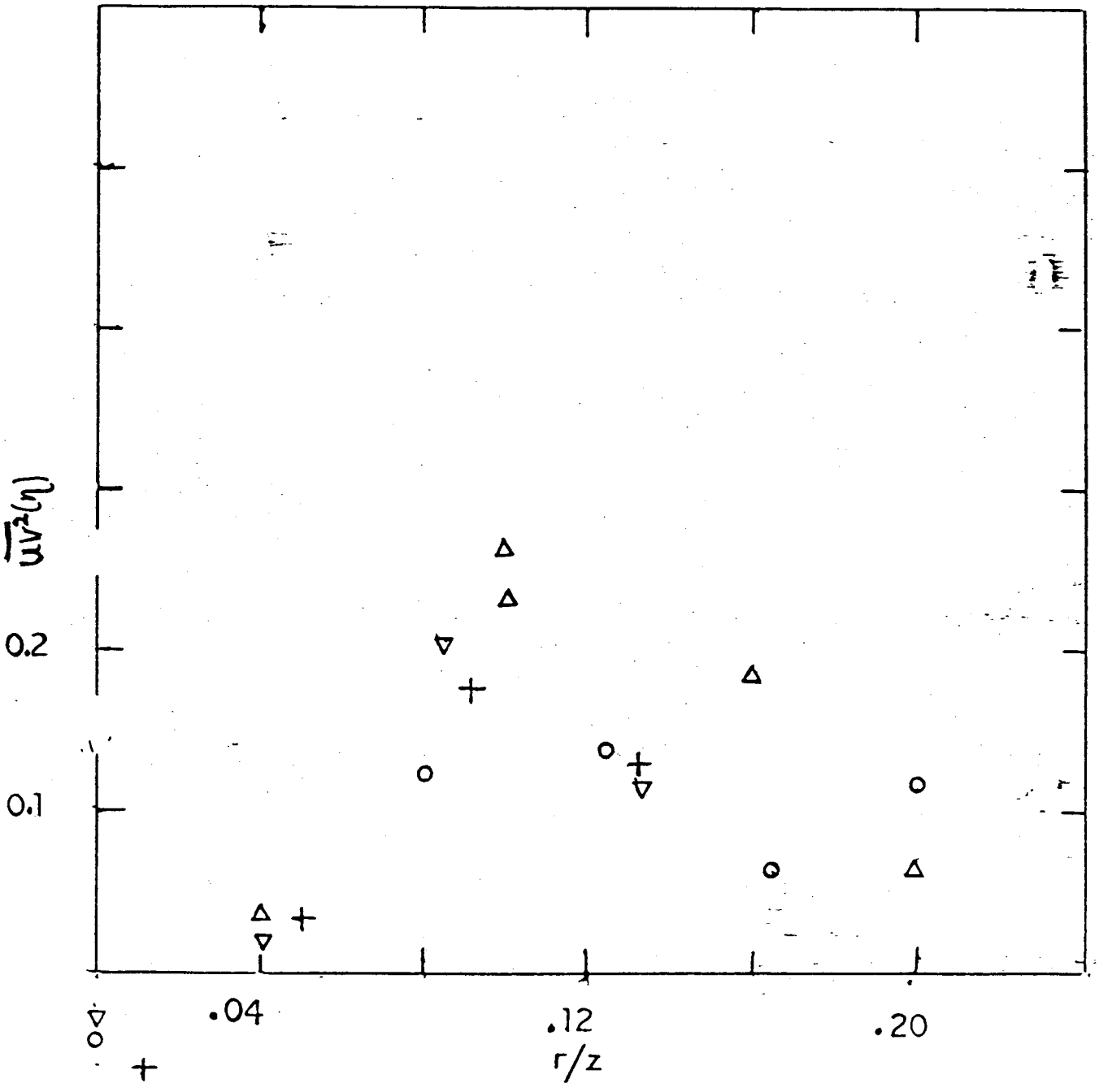

FIGURE 38

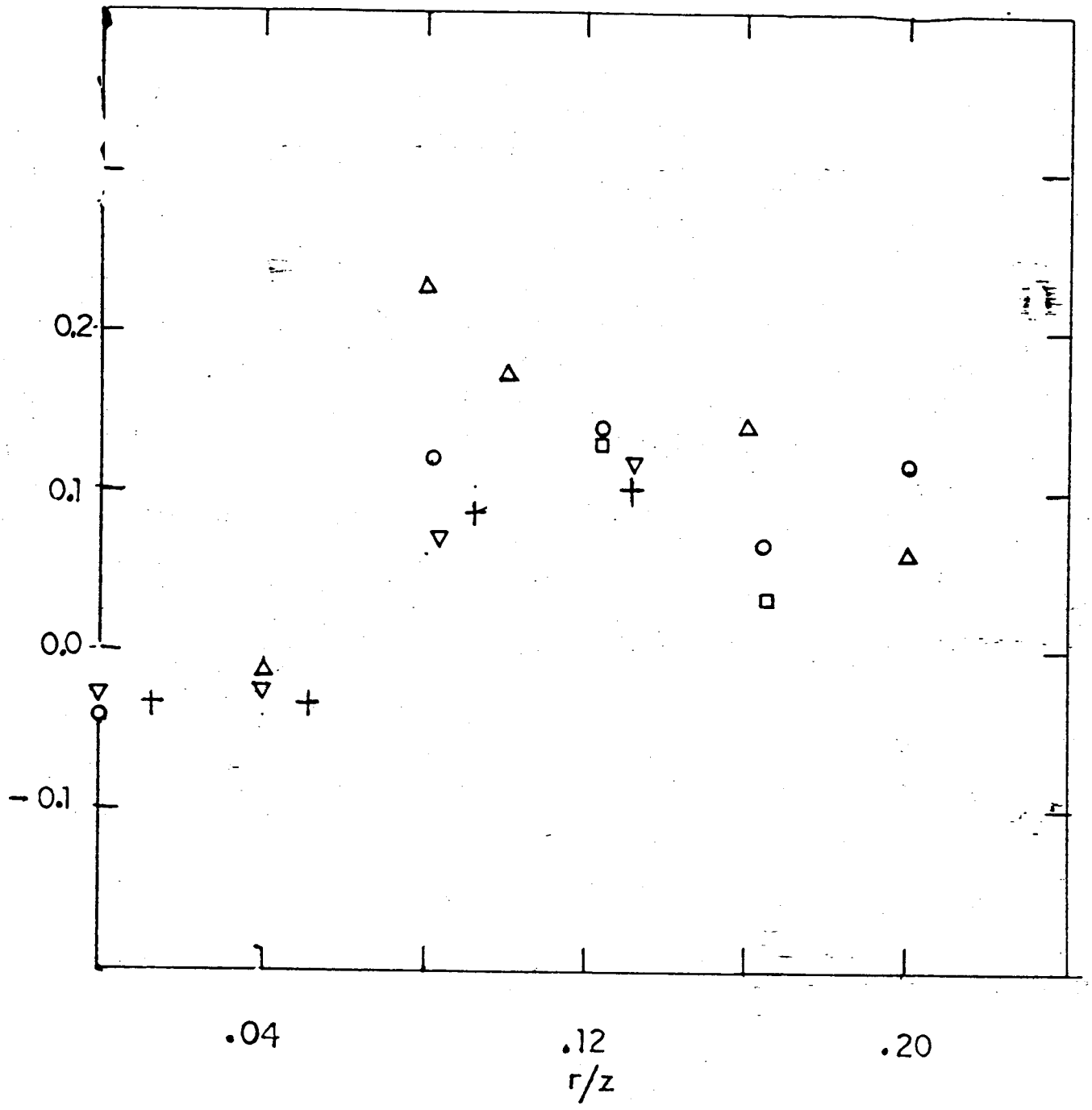

FIGURE 39

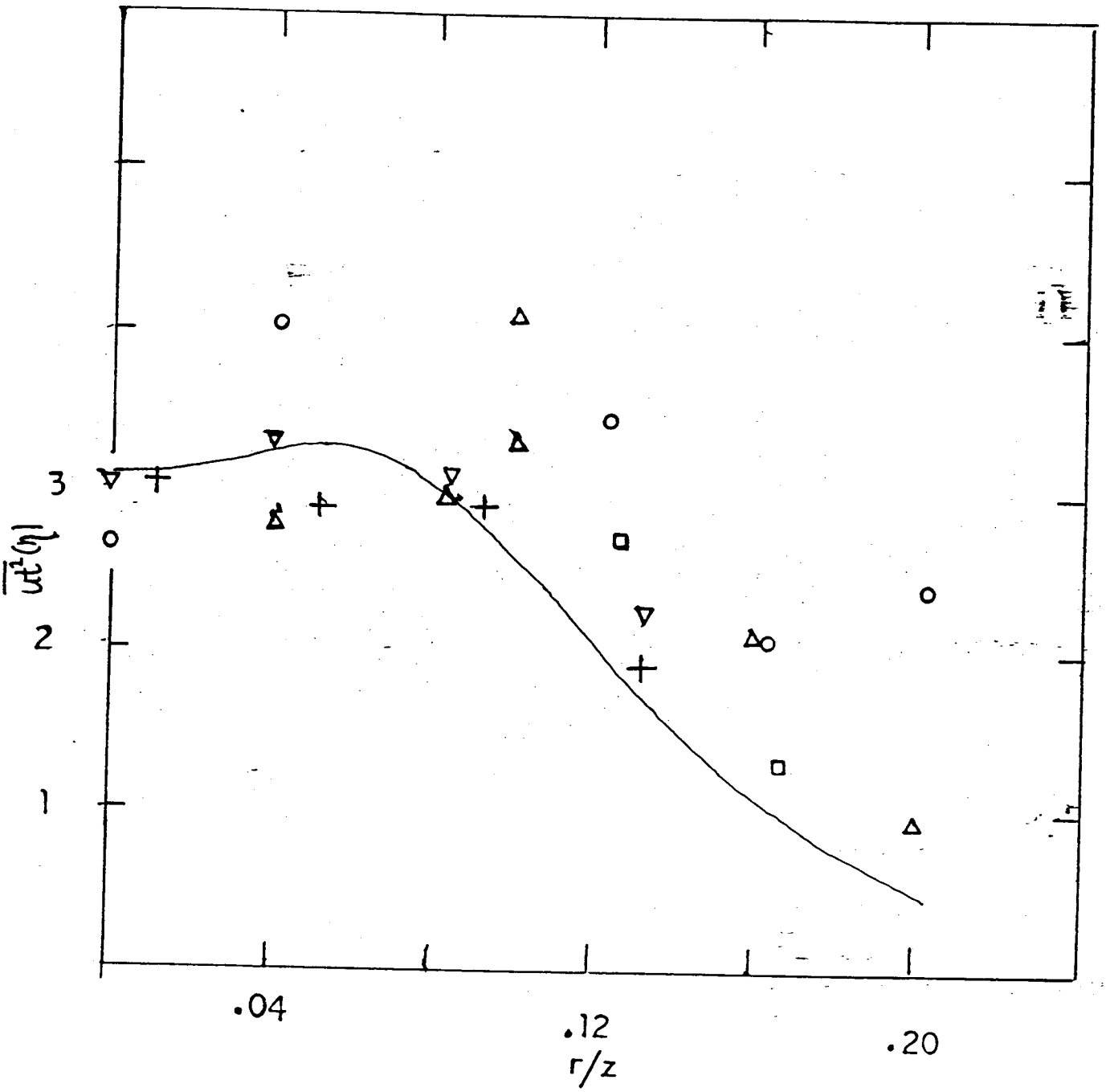

FIGURE 40

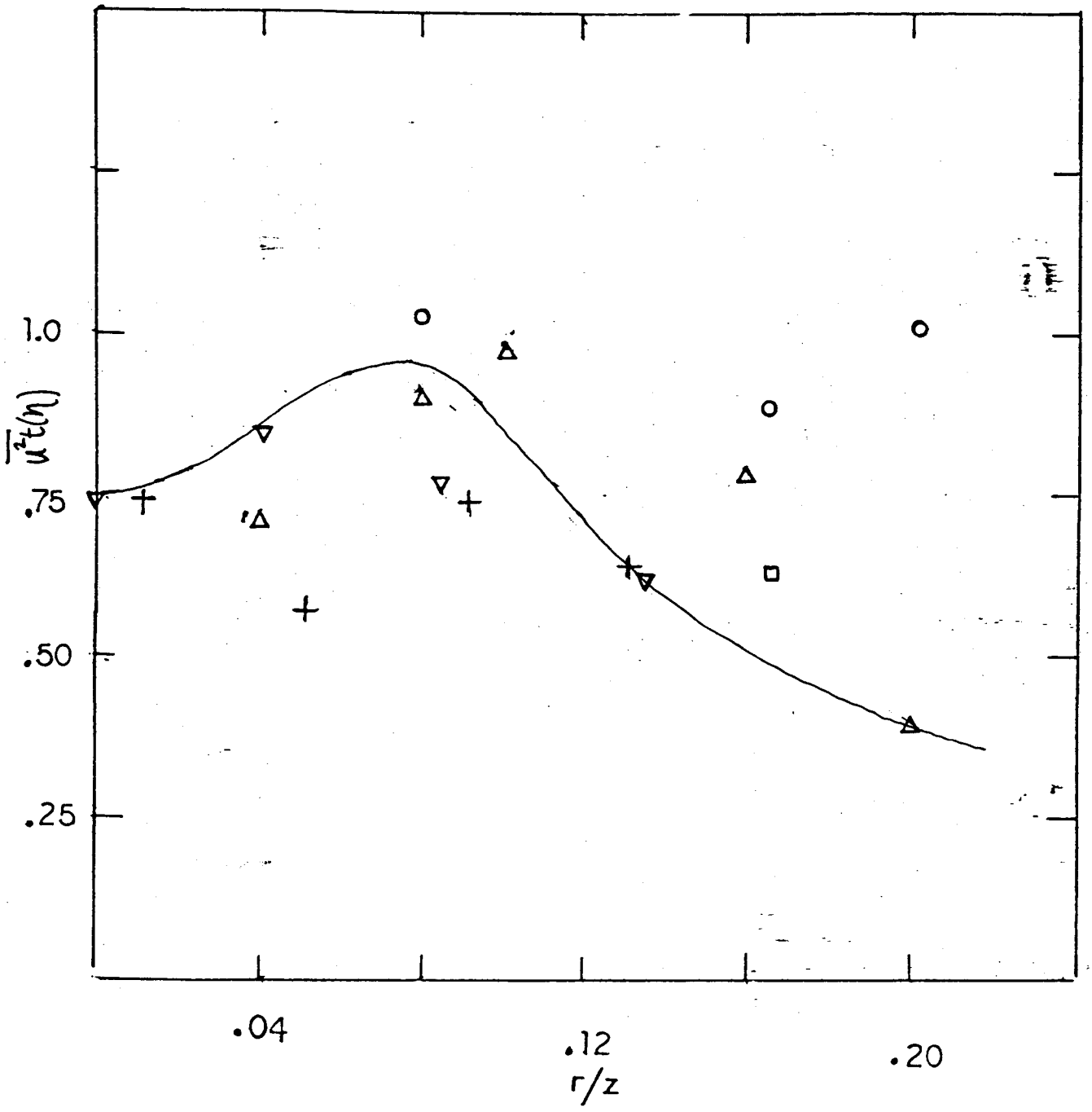

FIGURE 41